To date, several studies including the present one have demonstrated that IPI score remains predictive in the rituximab era, in contrast to biomarkers [18, 22, 23]. In the present study, the IPI system identified only two risk groups instead of four among our patients—a low and low-intermediate group and a high and high-intermediate group—as reported in previous studies [22, 23].

The addition of rituximab to chemotherapy has improved the outcome of patients. We and others have shown that OS now exceeds 50% even in the groups with unfavorable indicators [14–18, 22, 23], although some patients still have a very poor outcome. Therefore, other predictive factors must be characterized in order to identify patients who should receive alternative initial therapy. A number of molecular prognostic markers have already been identified in patients with DLBCL [30]. These markers now need to be reevaluated in the rituximab era to identify patients with unfavorable prognostic factors and to devise adequate treatment strategies.

In conclusion, we have demonstrated that a high serum SIL-2R level is an indicator of poor prognosis in DLBCL patients receiving rituximab combination chemotherapy. To accurately confirm whether serum SIL-2R influences the outcome of patients receiving rituximab combination chemotherapy, prospective investigation with long-term follow-up will be required.

acknowledgements

references

1. Jaffe ES, Harris NL, Stein H, Vardiman JW (eds): World Health Organization Classification of Tumours. Pathology and Genetics of Tumours of Haematopoietic and Lymphoid Tissue. IARC press 2001.

2. TIN-HsLPF. A predictive model for aggressive non-Hodgkin's lymphoma. The International Non-Hodgkin's Lymphoma Prognostic Factors Project. N Engl J Med 1993; 329: 987–994.

3. Gause A, Jung W, Schmits R et al. Soluble CD8, CD25 and CD30 antigens as prognostic markers in patients with untreated Hodgkin's lymphoma. Ann Oncol 1992; 3 (Suppl 4): 49–52.

4. Chilosi M, Semenzato G, Cetto G et al. Soluble interleukin-2 receptors in the sera of patients with hairy cell leukemia: relationship with the effect of recombinant alpha-interferon therapy on clinical parameters and natural killer in vitro activity. Blood 1987; 70: 1530–1535.

5. Wagner DK, Kiwanuka J, Edwards BK et al. Soluble interleukin-2 receptor levels in patients with undifferentiated and lymphoblastic lymphomas: correlation with survival. J Clin Oncol 1987; 5: 1262–1274.

6. Kamihira S, Atogami S, Sohda H et al. Significance of soluble interleukin-2 receptor levels for evaluation of the progression of adult T-cell leukemia. Cancer 1994; 73: 2753–2758.

7. Niitsu N, Iijima K, Chizuka A. A high serum-soluble interleukin-2 receptor level is associated with a poor outcome of aggressive non-Hodgkin's lymphoma. Eur J Haematol 2001; 66: 24–30.

8. Nakase K, Tsuji K, Tamaki S et al. Elevated levels of soluble interleukin-2 receptor in serum of patients with hematological or non-hematological malignancies. Cancer Detect Prev 2005; 29: 256–259.

9. Takeshita T, Asao H, Ohtani K et al. Cloning of the gamma chain of the human IL-2 receptor. Science 1992; 257: 379–382.

10. Rubin LA, Nelson DL. The soluble interleukin-2 receptor: biology, function, and clinical application. Ann Intern Med 1990; 113: 619–627.

11. Smith KA. Interleukin-2: inception, impact, and implications. Science 1988; 240: 1169–1176.

12. Voss SD, Sondel PM, Robb RJ. Characterization of the interleukin 2 receptors (IL-2R) expressed on human natural killer cells activated in vivo by IL-2: association of the p64 IL-2R gamma chain with the IL-2R beta chain in functional intermediate-affinity IL-2R. J Exp Med 1992; 176: 531–541.

13. Fisher RI, Gaynor ER, Dahlberg S et al. Comparison of a standard regimen (CHOP) with three intensive chemotherapy regimens for advanced non-Hodgkin's lymphoma. N Engl J Med 1993; 328: 1002–1006.

14. Coiffier B, Lepage E, Briere J et al. CHOP chemotherapy plus rituximab compared with CHOP alone in elderly patients with diffuse large-B-cell lymphoma. N Engl J Med 2002; 346: 235–242.

15. Habermann TM, Weller EA, Morrison VA et al. Rituximab-CHOP versus CHOP alone or with maintenance rituximab in older patients with diffuse large B-cell lymphoma. J Clin Oncol 2006; 24: 3121–3127.

16. Pfreundschuh M, Trumper L, Osterborg A et al. CHOP-like chemotherapy plus rituximab versus CHOP-like chemotherapy alone in young patients with good-prognosis diffuse large-B-cell lymphoma: a randomised controlled trial by the MabThera International Trial (MInT) Group. Lancet Oncol 2006; 7: 379–391.

17. Sehn LH, Donaldson J, Chhanabhai M et al. Introduction of combined CHOP plus rituximab therapy dramatically improved outcome of diffuse large B-cell lymphoma in British Columbia. J Clin Oncol 2005; 23: 5027–5033.

18. Sehn LH, Berry B, Chhanabhai M et al. The revised International Prognostic Index (R-IPI) is a better predictor of outcome than the standard IPI for patients with diffuse large B-cell lymphoma treated with R-CHOP. Blood 2007; 109: 1857–1861.

19. Gascoyne RD, Adomat SA, Krajewski S et al. Prognostic significance of Bcl-2 protein expression and Bcl-2 gene rearrangement in diffuse aggressive non-Hodgkin's lymphoma. Blood 1997; 90: 244–251.

20. Barrans SL, O'Connor SJ, Evans PA et al. Rearrangement of the BCL6 locus at 3q27 is an independent poor prognostic factor in nodal diffuse large B-cell lymphoma. Br J Haematol 2002; 117: 322–332.

21. Hans CP, Weisenburger DD, Greiner TC et al. Confirmation of the molecular classification of diffuse large B-cell lymphoma by immunohistochemistry using a tissue microarray. Blood 2004; 103: 275–282.

22. Winter JN, Weller EA, Horning SJ et al. Prognostic significance of Bcl-6 protein expression in DLBCL treated with CHOP or R-CHOP: a prospective correlative study. Blood 2006; 107: 4207–4213.

23. Nyman H, Adde M, Karjalainen-Lindsberg ML et al. Prognostic impact of immunohistochemically defined germinal center phenotype in diffuse large B-cell lymphoma patients treated with immunochemotherapy. Blood 2007; 109: 4930–4935.

24. Wilson H, Pittaluga S, O'Connor P. Rituximab may overcome Bcl-2-associated chemotherapy resistance in untreated diffuse large B-cell lymphomas [abstract]. Blood 2001; 98: 343a.

25. Cheson BD, Horning SJ, Coiffier B et al. Report of an international workshop to standardize response criteria for non-Hodgkin's lymphomas. NCI Sponsored International Working Group. J Clin Oncol 1999; 17: 1244.

26. Ogura M, Morishima Y, Kagami Y et al. Randomized phase II study of concurrent and sequential rituximab and CHOP chemotherapy in untreated indolent B-cell lymphoma. Cancer Sci 2006; 97: 305–312.

27. Davis RE, Brown KD, Siebenlist U, Staudt LM. Constitutive nuclear factor kappaB activity is required for survival of activated B cell-like diffuse large B cell lymphoma cells. J Exp Med 2001; 194: 1861–1874.

28. Jazirehi AR, Bonavida B. Cellular and molecular signal transduction pathways modulated by rituximab (rituxan, anti-CD20 mAb) in non-Hodgkin's lymphoma:

implications in chemosensitization and therapeutic intervention. Oncogene 2005; 24: 2121–2143.

29. Jazirehi AR, Huerta-Yepez S, Cheng G, Bonavida B. Rituximab (chimeric anti-CD20 monoclonal antibody) inhibits the constitutive nuclear factor-(kappa)B signaling pathway in non-Hodgkin's lymphoma B-cell lines: role in sensitization to chemotherapeutic drug-induced apoptosis. Cancer Res 2005; 65: 264–276.

30. Lossos IS, Morgensztern D. Prognostic biomarkers in diffuse large B-cell lymphoma. J Clin Oncol 2006; 24: 995–1007.

SRPX2 is overexpressed in gastric cancer and promotes cellular migration and adhesion

Kaoru Tanaka[1,2], Tokuzo Arao[1], Mari Maegawa[1], Kazuko Matsumoto[1], Hiroyasu Kaneda[1,2], Kanae Kudo[1], Yoshihiko Fujita[1], Hideyuki Yokote[1], Kazuyoshi Yanagihara[3], Yasuhide Yamada[4], Isamu Okamoto[2], Kazuhiko Nakagawa[2] and Kazuto Nishio[1]*

[1]*Department of Genome Biology, Kinki University School of Medicine, Osaka-Sayama, Osaka, Japan*
[2]*Department of Medical Oncology, Kinki University School of Medicine, Osaka-Sayama, Osaka, Japan*
[3]*Central Animal Lab, National Cancer Center Research Institute, Chuo-ku, Tokyo, Japan*
[4]*Department of Medical Oncology, National Cancer Center Hospital, Chuo-ku, Tokyo, Japan*

SRPX2 (Sushi repeat containing protein, X-linked 2) was first identified as a downstream molecule of the *E2A-HLF* fusion gene in t(17;19)-positive leukemia cells and the biological function of this gene remains unknown. We found that *SRPX2* is overexpressed in gastric cancer and the expression and clinical features showed that high mRNA expression levels were observed in patients with unfavorable outcomes using real-time RT-PCR. The cellular distribution of SRPX2 protein showed the secretion of SRPX2 into extracellular regions and its localization in the cytoplasm. The introduction of the *SRPX2* gene into HEK293 cells did not modulate the cellular proliferative activity but did enhance the cellular migration activity, as shown using migration and scratch assays. The conditioned-medium obtained from SRPX2-overexpressing cells increased the cellular migration activity of a gastric cancer cell line, SNU-16. In addition, SRPX2 protein remarkably enhanced the cellular adhesion of SNU-16 and HSC-39 and increased the phosphorylation levels of focal adhesion kinase (FAK), as shown using western blotting, suggesting that SRPX2 enhances cellular migration and adhesion through FAK signaling. In conclusion, the overexpression of SRPX2 enhances cellular migration and adhesion in gastric cancer cells. Here, we report that the biological functions of SRPX2 include cellular migration and adhesion to cancer cells.
© 2008 Wiley-Liss, Inc.

Key words: SRPX2; gastric cancer; cellular adhesion; cellular migration

SRPX2 (Sushi repeat containing protein, X-linked 2) was first identified as *SRPUL* (Sushi repeat protein upregulated in leukemia) by Kurosawa *et al.*[1] The *E2A-HLF* fusion gene causes B-cell precursor acute lymphoblastic leukemia, which is characterized by an unusual paraneoplastic syndrome comprising intravascular coagulation and hypercalcemia; one of the target genes of *E2A-HLF* is *SRPX2*. Apart from the possible involvement of this gene in malignant diseases, a disease-causing mutation (p.N327S) in *SRPX2* resulting in a gain-of-glycosylation aberration in the secreted mutant protein, and the mutation actually leads to rolandic epilepsy with oral and speech dyspraxia and with mental retardation in the French family.[2] While a second mutation (p.Y72S) leads to rolandic epilepsy with bilateral perisylvian polymicrogyria in another family.[3] The involvement of *SRPX2* in these disorders suggests an important role for *SRPX2* in the perisylvian region, which is critical for language and cognitive development.

SRPX2 contains 3 sushi domains and 1 hyaline domain. A sushi domain, also known as a complement control protein module or a short complement-like repeat, contains ~60 amino acids and is found in functionally diverse proteins, such as regulators of the complement activation family, GABA receptor, thyroid peroxidase and selectin family.[4,5] Sushi domains are thought to mediate specific protein–protein or protein–carbohydrate binding and cellular adhesive functions.[4] A phylogenetic analysis revealed that *SRPX2* belongs to a family of 5 genes: *SRPX2, SRPX, SELP* (selectin P precursor), *SELE* (selectin E precursor) and *SVEP1* (selectin-like protein).[3] *SRPX/SRPX1/EXT1/DRS* has the highest degree of similarity and may be involved in X-linked retinitis pigmentosa.[6,7] The selectin family, which is well known for its

biological roles in leukocyte migration, cellular attachment and rolling, also contains sushi domain repeats and are phylogenetic similar to *SRPX2*.[3]

SRPX2 also contains a hyaline (HYR) domain, and this domain probably corresponds to a new superfamily in the immunoglobulin fold. The HYR domains are often associated with sushi domains, and although the function of HYR domains is uncertain, it is thought to be involved in cellular adhesion.[8] Thus, accumulating data on the motifs found in *SRPX2* suggest that *SRPX2* may be involved in cellular adhesion.

We previously performed a microarray analysis of paired clinical samples of gastric cancer and noncancerous lesions obtained from gastric cancer patients[9] and found that *SRPX2* is overexpressed in gastric cancer tissue. The present study sought to clarify the biological function of *SRPX2* expression in gastric cancer.

Material and methods

Cell culture

HEK293 (human embryonic kidney cell line) was maintained in DMEM medium, and SNU-16, HSC-39, 44As3, HSC-43, HSC-44, MKN1 and MKN7 (human gastric cancer cell lines) were maintained in RPMI1640 medium (Sigma, St. Louis, MO) supplemented with 10% FBS (GIBCO BRL, Grand Island, NY). HUVEC (human umbilical vein endothelial cells) was maintained in Humedia-EG2 (KURABO, Tokyo, Japan) medium with 1% FBS under the addition of epidermal growth factor and fibroblast growth factor.

Expression vector construction and viral production

The full-length cDNA fragment encoding human *SRPX2* was obtained from 44As3 cells using RT-PCR and the following primers: SRPX2-F, CGG GAT CCT CAA GGA TGG CCA GTC AGC TAA CTC AAA GAG G; SRPX2-R, CCC AAG CTT GGG CTC GCA TAT GTC CCT TTG CTC CCG ACG CTG GG. The sequences of the PCR-amplified DNAs were confirmed by sequencing after cloning into a pCR-Blunt II-TOPO cloning vector (Invitrogen, Carlsbad, CA). *SRPX2* cDNA was fused to a GFP-containing pcDNA3.1 vector (Clontech, Palo Alt, CA). Empty, GFP and SRPX2-GFP vectors were then transfected into HEK293 cells using FuGENE6 transfection reagent (Roche Diagnostics, Basel, Switzerland). Hygromycin selection (100 μg/mL) was

performed on days 2–8 after transfection, and then the cells were cultured in normal medium for another 10 days. The vectors and stable transfectant HEK293 cells were designated as pcDNA-mock, pcDNA-GFP, pcDNA-SRPX2/GFP, HEK293-pcDNA-mock, HEK293-pcDNA-GFP and HEK293-pcDNA-SRPX2/GFP.

SRPX2 cDNA in pcDNA3.1 vector was cut out and transferred into a pQCLIN retroviral vector (BD Biosciences Clontech, San Diego, CA) together with enhanced green fluorescent protein (EGFP) following internal ribosome entry site sequence (IRES) to monitor the expression of the inserts indirectly. A pVSV-G vector (Clontech, Palo Alt, CA) for the constitution of the viral envelope and the pQCXIX constructs were cotransfected into the GP2-293 cells using FuGENE6 transfection reagent. Briefly, 80% confluent cells cultured on a 10-cm dish were transfected with 2 μg pVSV-G plus 6 μg pQCXIX vectors. After 48 hr of transfection, the culture medium was collected and the viral particles were concentrated by centrifugation at 15,000g for 3 hr at 4°C. The viral pellet was then resuspended in fresh RPMI1640 medium. The titer of the viral vector was calculated by counting the EGFP-positive cells that were infected by serial dilutions of virus-containing media, and the multiplicity of infection (MOI) was then determined. The viral vector and stable viral transfectant cells in each cell line were designated as pQCLIN-EGFP, pQCLIN-SRPX2, HEK293-pQCLIN-EGFP, HEK293-pQCLIN-SRPX2, MKN1-pQCLIN-EGFP and MKN1-pQCLIN-SRPX2.

Patients and samples

An analysis of SRPX2 expression levels and clinical features was performed using data from patients aged 20 to 75 years and with histologically confirmed, Stage IV gastric cancer. Additional inclusion criteria included an Eastern Cooperative Oncology Group performance status of 0–2. The exclusion criteria included prior chemotherapy or major surgery. Fifty-seven gastric cancer samples were evaluated in this study. All the patients received chemotherapy after registration and endoscopic biopsy. Gastric cancer and noncancerous gastric mucosa samples were evaluated for SRPX2 expression in the first consecutive 24 patients. This study was approved by the institutional review board of the National Cancer Center Hospital, and written informed consent was obtained from all the patients. Endoscopic biopsy samples were immediately placed in an RNA stabilization solution (Isogen; Nippongene, Tokyo, Japan) and stored at −80°C. Other biopsy samples obtained from the same location were reviewed by a pathologist to confirm the presence of tumor cells. The RNA extraction method and the quality check protocol have been previously described.[10]

Real-time reverse-transcription PCR

One microgram of total RNA from normal tissue purchased from Clontech and from a cultured cell line was converted to cDNA using a GeneAmp® RNA-PCR kit (Applied Biosystems, CA). Real-time PCR was carried out using the Applied Biosystems 7900HT Fast Real-time PCR System (Applied Biosystems) under the following conditions: 95°C for 6 min, 40 cycles of 95°C for 15 sec and 60°C for 1 min. Glyceraldehyde 3 phosphate dehydrogenase (GAPD, NM_002046) was used to normalize the expression levels in the subsequent quantitative analyses. To amplify the target genes, the following primers were purchased from TaKaRa (Yotsukaichi, Japan): SRPX2-FW, ACT GGA TTT GCG GCA TGT GA; SRPX2-RW, CCA TGT TGA AGT AGG AGC GAG TGA; GAPD-FW, GCA CCG TCA AGG CTG AGA AC; GAPD-RW, ATG GTG GTG AAG ACG CCA GT.

Anti-SRPX2 polyclonal antibody

Rabbit antibodies specific for SRPX2 were obtained by immunizing rabbits with SRPX2 peptide (FIDDYLLSNQELTQ) according to a previously described method.[2] and IgG was purified from serum using standard protocols.

SRPX2-conditioned medium

The media in which subconfluent HEK293-pQCLIN-EGFP, HEK293-pQCLIN-SRPX2, MKN1-pQCLIN-EGFP and MKN1-pQCLIN-SRPX2 cells were being cultured was replaced with a serum-reduced medium (OPTI-MEM; GIBCO), the cells were cultured for an additional 24 hr and the conditioned-media were collected. The media were filtered using Millex-GS (Millipore, Bedford, MA) and concentrated using the Amicon Ultra (Millipore) and stored at −80°C. The concentration of the conditioned-medium was measured using a BCA protein assay (Pierce Biotechnology, Rockford, IL) and equalized.

Western blot analysis

The antibodies used in this study were anti-GFP (Invitrogen, Carlsbad, CA), anti-focal adhesion kinase (anti-FAK), anti-p-FAK (pY397) (BD Biosciences), anti-β-actin (Santa Cruz Biotechnology, Santa Cruz, CA) and anti-p-FAK (pY576/577) (Cell Signaling, Beverly, MA).

A Western blot analysis was performed as described previously (Ref. 10). In brief, subconfluent cells were washed with cold phosphate-buffered saline (PBS) and harvested with Lysis A buffer containing 1%Triton X-100, 20 mM Tris-HCl (pH 7.0), 5 mM EDTA, 50 mM sodium chloride, 10 mM sodium pyrophosphate, 50 mM sodium fluoride, 1 mM sodium orthovanadate and a protease inhibitor mix, complete™ (Roche Diagnostics). Whole-cell lysates and culture medium were separated using a 2–15% gradient SDS-PAGE and blotted onto a polyvinylidene fluoride membrane. After blocking with 3% bovine serum albumin in a TBS buffer (pH 8.0) with 0.1% Tween-20, the membrane was probed with primary antibody. After rinsing twice with TBS buffer, the membrane was incubated with horseradish peroxidase-conjugated secondary antibody (Cell Signaling) and washed followed by visualization using an ECL detection system (Amersham) and LAS-3000 (Fujifilm, Tokyo, Japan). The data were quantified by automated densitometry using Multigauge Ver 3.0 (Fujifilm).The experiment was performed in triplicate.

Cellular growth assay

HEK293 transfectant cells were incubated on 96-well plates at a density of 2000/well with 180 μL of culture medium at 37°C in 5% CO_2. After 24, 48 or 72 hr of incubation, 20 μL of MTT [3-(4,5-dimethyl-thiazoyl-2-yl)2,5-diphenyltetrazolium bromide] solution (SIGMA) was added and the cultures were incubated for 4 hr at 37°C. After centrifugation, the culture medium was discarded and the wells were filled with DMSO. The absorbance of the cultures at 562 nm was measured using VERSAmax (Japan Molecular Devices, Tokyo, Japan). The experiment was performed in triplicate.

Cellular adhesion assay

EGFP-conditioned or SRPX2-conditioned media obtained from HEK293-pQCLIN-EGFP, HEK293-pQCLIN-SRPX2, MKN1-pQCLIN-EGFP or MKN1-pQCLIN-SRPX2 cells were adjusted to a concentration of 1 mg/mL and 50 μL were incubated at 4°C overnight on 96-well plates. The conditioned media were aspirated, and the wells were washed twice with PBS. The plates were then used in an adhesion assay as conditioned medium-coated 96-well plates. The cells to be analyzed were added to the wells of conditioned medium-coated plates (2×10^4 cells /well) and incubated at 37°C for 1 hr. When treated with FAK inhibitors (PP2 and Herbimycin A; Calbiochem, San Diego, CA), the cells to be analyzed were incubated for 4 hr. The wells were then washed twice with PBS to remove nonadherent cells. Adherent cells were evaluated using the MTT assay as described above. The average O.D. values of 3 wells were used for a single experiment, and the experiment was performed in triplicate.

Migration assay and chemotaxis assay

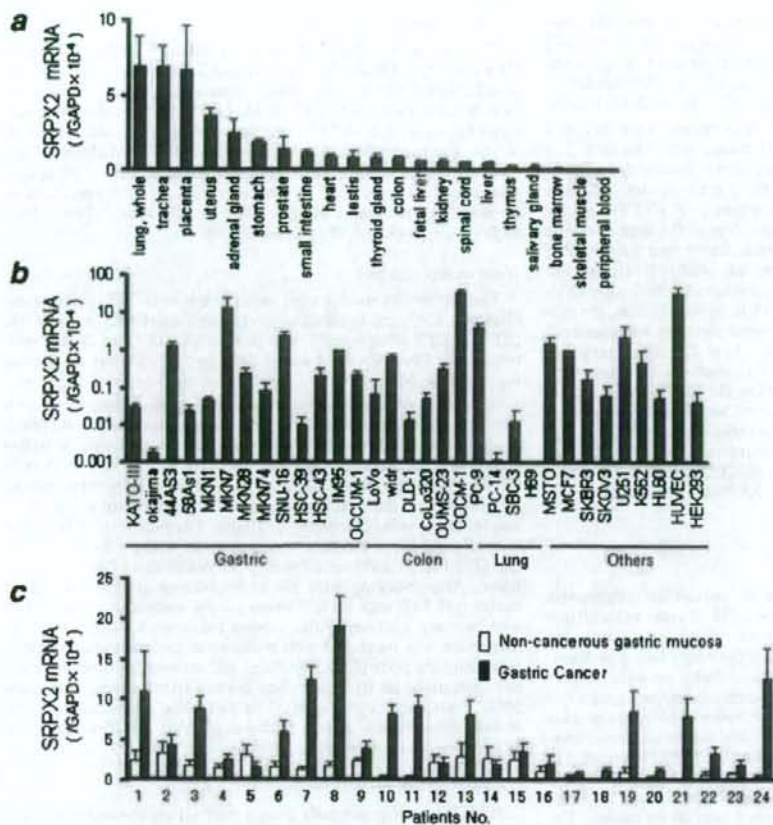Migration assays were performed using the Boyden-chamber methods and polycarbonate membranes with an 8-μm pore size

(chemotaxicell; KURABO). The membranes were coated with fibronectin on the outer side and dried for 2 hr at room temperature. The cells to be analyzed (2×10^4/well) were then seeded onto the upper chambers with 200 μL of migrating medium (DMEM containing 0.5% FBS), and the upper chambers were placed into the lower chambers of 24-well culture dishes containing 600 μL of DMEM containing 10% FBS. After incubation for 8 hr at 37°C, the media in the upper chambers were aspirated and the nonmigrated cells on the inner sides of the membranes were removed using a cotton swab. The cells that had migrated to the outer side of the membranes were fixed with 4% paraformaldehyde for 10 min and stained with 0.1% crystal violet for 15 min, then counted using a light microscope. The experiment was performed in triplicate.

The chemotaxis assays were performed using SNU-16 cells. A total of 1×10^5 cells were seeded onto the upper chambers with 200 μL of RPMI containing 0.5% FBS. The final concentration at 100 μg/mL of EGFP-conditioned or SRPX2-conditioned medium was added to the 600 μL volume of RPMI1640 containing 0.5% FBS medium in the lower chamber of the 24-well culture dishes. The cells were then incubated for 24 hr at 37°C with 5% CO_2. The number of migrated cells was evaluated as described earlier. The experiment was performed in triplicate.

Wound healing assay

HEK293-pQCLIN-EGFP and HEK293-pQCLIN-SRPX2 cells were plated onto 3.5-cm dishes and incubated in DMEM containing 10% FBS until they reached confluence. Wounds were introduced to the confluent cell monolayer using a plastic pipette tip.

The cells were then cultured with DMEM containing 10% FBS at 37°C. After 4, 8 and 12 hr later, the wound area was photographed using a light microscope and measured. The experiment was performed in triplicate.

Fluorescent microscopy

HEK293-pcDNA-GFP and HEK293-pcDNA-SRPX2/GFP cells were treated with DAPI (6-diamidino-2-phenylindole) to stain the nucleus and photographed using fluorescent microscopy, IX71 (Olympus, Tokyo, Japan).

Statistics

The *t* test was used for comparison between 2 groups and paired *t* test was used for paired-samples in Figure 1*c*. The statistical analysis was performed using Excel software (Microsoft, Redmond, WA). A *p* value < 0.05 was considered significant.

Results

Tissue distribution of SRPX2 mRNA in normal tissues and cell lines

To examine the tissue distribution of *SRPX2* mRNA, we performed real-time RT-PCR for 24 normal human tissues. High expression levels of *SRPX2* mRNA were detected in the placenta, lung, trachea, uterus and adrenal gland, whereas the levels in the peripheral blood, brain and bone marrow were relatively low (Fig. 1*a*). Combined with data from previous reports,[1,2] *SRPX2* mRNA

appears to be widely observed in normal tissues, with particularly high levels detected in the placenta and lung.

SRPX2 expression was also examined in 30 human cancer cell lines, HUVEC and HEK293 cells. A relatively high *SRPX2*

mRNA expression level was observed in gastric cancer (44As3, MKN7 and SNU-16), colorectal cancer (WiDr and COCM-1), lung cancer (PC-9), mesothelioma (MSTO), glioma (U251) and HUVEC. These results suggest that a variety of cancer and vascular endothelial cells express *SRPX2* (Fig. 1b).

Overexpression of SRPX2 mRNA in gastric cancer tissues

The expression of *SRPX2* mRNA was analyzed for paired tissues of gastric cancer and noncancerous gastric mucosa obtained from 24 gastric cancer patients. A paired *t* test demonstrated that *SRPX2* expression was significantly increased ($p = 0.0004$) in the cancerous tissues, compared to the noncancerous gastric mucosa (Fig. 1c). The *SRPX2* mRNA expression levels in the gastric cancer and noncancerous gastric mucosa were 6.6 ± 5.4 and 1.8 ± 1.2 ($\times 10^{-4}/GAPD$), respectively. Although the reason is unclear, 2 groups seemed to be present: 1 group with very high expression levels in cancerous tissues and another group with no difference in the expression levels between cancerous and noncancerous lesions.

To clarify the clinical significance of *SRPX2* expression, we examined the expression in an additional 57 gastric cancer samples using real-time RT-PCR and analyzed the correlations between *SRPX2* expression and clinical characteristics (Table I). Age, sex and histological cancer type were not correlated with *SRPX2* expression. However, patients with an unfavorable outcome, in whom the overall survival time (OS) was less than 6 months, exhibited significantly high expression levels of *SRPX2* in
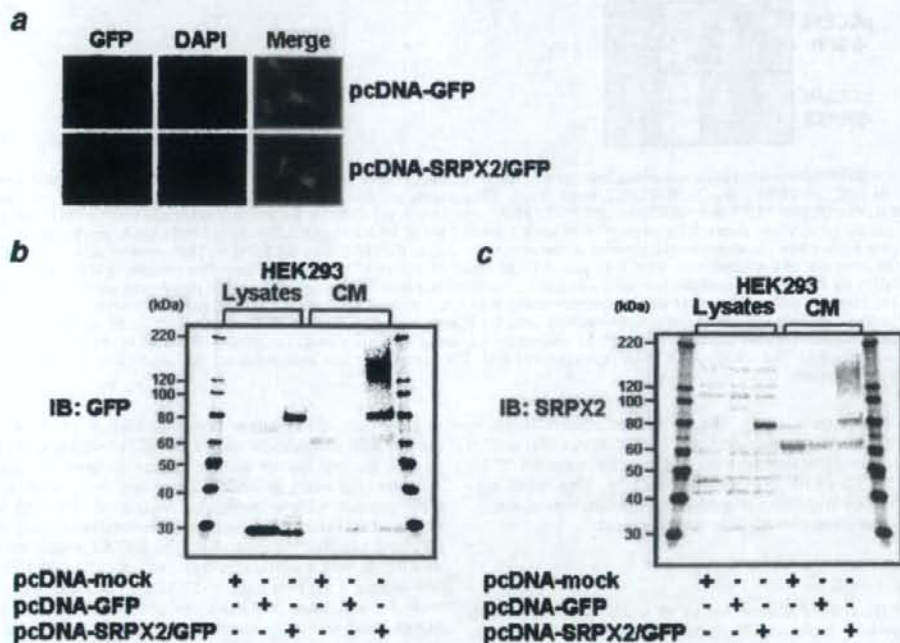
TABLE I – *SRPX2* EXPRESSION AND PATIENT CHARACTERISTICS IN PATIENTS WITH GASTRIC CANCER

Characteristics	Patients No. (%)	SRPX2	
		Expression ($10^{-4}/GAPD$)	p value
Age, years			
≥60	31 (54)	12.6 ± 12.5	0.10
<60	26 (46)	11.1 ± 9.1	
Sex			
Male	41 (72)	11.1 ± 9.1	0.61
Female	16 (28)	12.6 ± 12.5	
Histology[1]			
Diff.	22 (39)	11.3 ± 7.9	0.77
Undiff.	32 (56)	12.2 ± 11.7	
Prognosis[2]			
Favorable (>6 months)	37 (65)	9.5 ± 7.2	<0.05
Unfavorable (<6 months)	20 (35)	15.1 ± 13.5	
Total	57		

[1]Histology of endoscopic samples divided into differentiated and undifferentiated type.–[2]Overall survival time from the first day of chemotherapy. A survival time of 6 months was used as the cut-off to divide patients into "Favorable" and "Unfavorable" groups.

FIGURE 2 – Cellular distribution of SRPX2-GFP fusion protein. To examine the cellular distribution of SRPX2, we created cell lines expressing a fusion protein of SRPX2-GFP. The empty vector, GFP and SRPX2-GFP vectors were transfected into HEK293 cells using FuGENE6 transfection reagent. The vectors and stable transfectant cells in the HEK293 cells were designated as pcDNA-mock, pcDNA-GFP, pcDNA-SRPX2/GFP, HEK293-pcDNA-mock, HEK293-pcDNA-GFP and HEK293-pcDNA-SRPX2/GFP. (*a*) Fluorescence microscopy of HEK293-pcDNA-GFP (upper panel) and pcDNA-SRPX2/GFP cells (lower panel). The SRPX2/GFP fusion protein (green) showed a cytoplasmic distribution. The nucleus was stained by DAPI (blue). Western blot analysis detected by (*b*) anti-GFP antibody and (*c*) anti-SRPX2 antibody for HEK293-pcDNA-mock, HEK293-pcDNA-GFP and HEK293- pcDNA-SRPX2/GFP cells. Both the anti-GFP and the anti-SRPX2 antibodies detected the SRPX2-GFP fusion protein at ~80 kDa in the cell lysate and the secreted form at 150–180 kDa. IB, immunoblot; CM, culture medium.
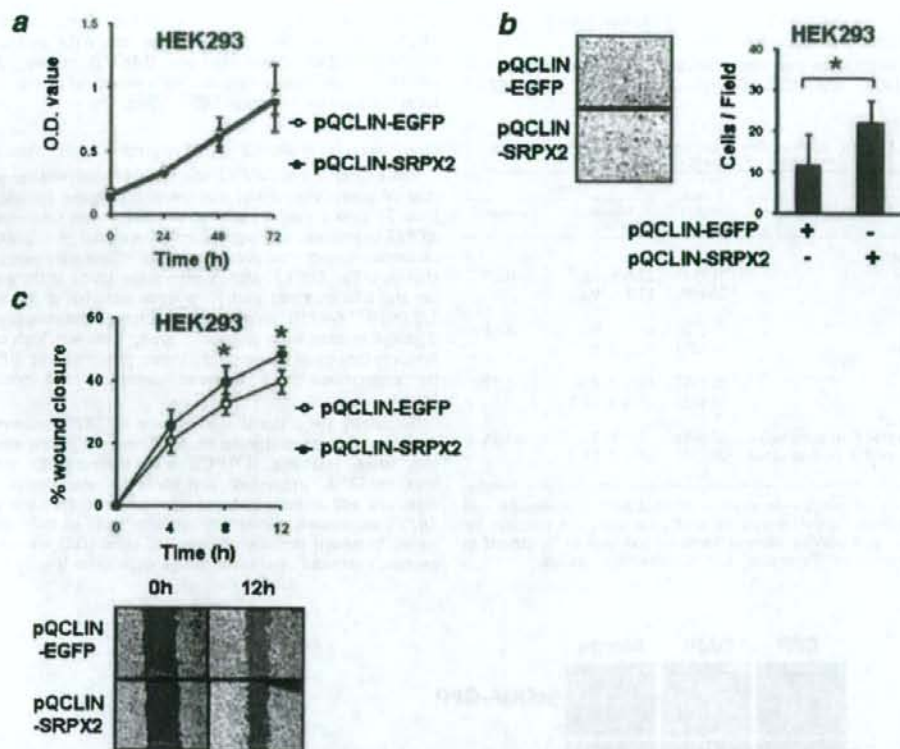
FIGURE 3 – SRPX2-introduced cells enhanced cellular migration but not cellular growth. Viral vectors containing EGFP and SRPX2 were constructed as pQCLIN-EGFP and pQLIN-SRPX2, respectively. These stable cell lines, retrovirally introduced into HEK293 cells, were designated as HEK293-pQCLIN-EGFP and HEK293-pQCLIN-SRPX2, respectively. (a) Cellular growth was examined using an MTT assay. No difference in cellular growth was observed between HEK293-pQCLIN-EGFP and HEK293-pQCLIN-SRPX2 cells. (b) Migration assay. Cells (2 × 10⁴/well) were seeded into the upper chambers with serum-reduced medium (DMEM with 0.5% FBS). The upper chambers, with fibronectin coated on the outer side of the membrane, were then placed in the lower chambers of a 24-well culture plate containing DMEM with 10% FBS. After incubation for 8 hr at 37°C, medium was aspirated and the nonmigrated cells on the inner side of the membrane were removed using a cotton swab. The migrated cells on the outer side of the membrane were fixed, stained and counted using a light microscope. The experiment was performed in triplicate. The left panels show representative data. (c) Wound healing assay for HEK293-pQCLIN-EGFP and HEK293-pQCLIN-SRPX2 cells. Wounds were introduced to the confluent cell monolayer using a plastic pipette tip. After 4, 8 and 12 hr, the wound area was photographed and measured. The lower panels show representative data. The experiment was performed in triplicate. *: $p < 0.05$. EGFP, enhanced green fluorescent protein.

cancerous tissues ($p < 0.05$). The SRPX2 expression levels in patients with an unfavorable outcome (OS < 6 months) and in those with a favorable outcome (OS > 6 months) were 9.5 ± 7.2 and 15.1 ± 13.5 (×10⁻⁴/GAPD), respectively. This result suggests that SRPX2 might be a prognostic biomarker, that is, associated with a malignant phenotype in gastric cancer.

SRPX2 is secreted into culture medium and localized in cytoplasm

Because the cellular distribution of an uncharacterized protein often suggest its biological function (e.g., transcription factors tend to be localized in the nucleus), we tried to identify the cellular distribution of SRPX2 using a SRPX2-GFP fusion protein. We introduced an empty vector, GFP, or SRPX2 fused with GFP into HEK293 cells to create the following stable cell lines: HEK293-pcDNA-mock, HEK293-pcDNA-GFP and HEK293- pcDNA-SRPX2/GFP, respectively. The SRPX2-GFP fusion protein exhibited a cytoplasmic distribution (Fig. 2a). The protein expression of SRPX2 was then analyzed using western blotting and both anti-GFP and anti-SRPX2 antibodies (Figs. 2b and 2c). Western blot-

ting with anti-GFP antibody revealed that an SRPX2-GFP fusion protein with a molecular weight (M.W.) of ~80 kDa was detected in both the cell lysates and the culture medium. A similar result was observed using anti-SRPX2 antibody. In addition, an SRPX2/GFP protein with a molecular weight of 150–180 kDa was observed in the culture medium when analyzed using both anti-GFP and anti-SRPX2 antibodies. The SRPX2 protein was detected as 2 bands with molecular weights of ~80 kDa and 150–180 kDa (containing a GFP protein of 30 kDa). The band was consistent with the estimated molecular weight of SRPX2, 53 kDa. The higher band was only observed in the culture medium and was detected using both anti-GFP and anti-SRPX2 antibodies.

SRPX2-introduced cells enhanced cellular migration but not cellular growth

To elucidate the biological function of SRPX2, EGFP or SRPX2 was retrovirally introduced into HEK293 cells. The stable cell lines were designated as HEK293-pQCLIN-EGFP and HEK293-pQCLIN-SRPX2, respectively. We then performed cellular growth assays using these cells (Fig. 3a). No difference in
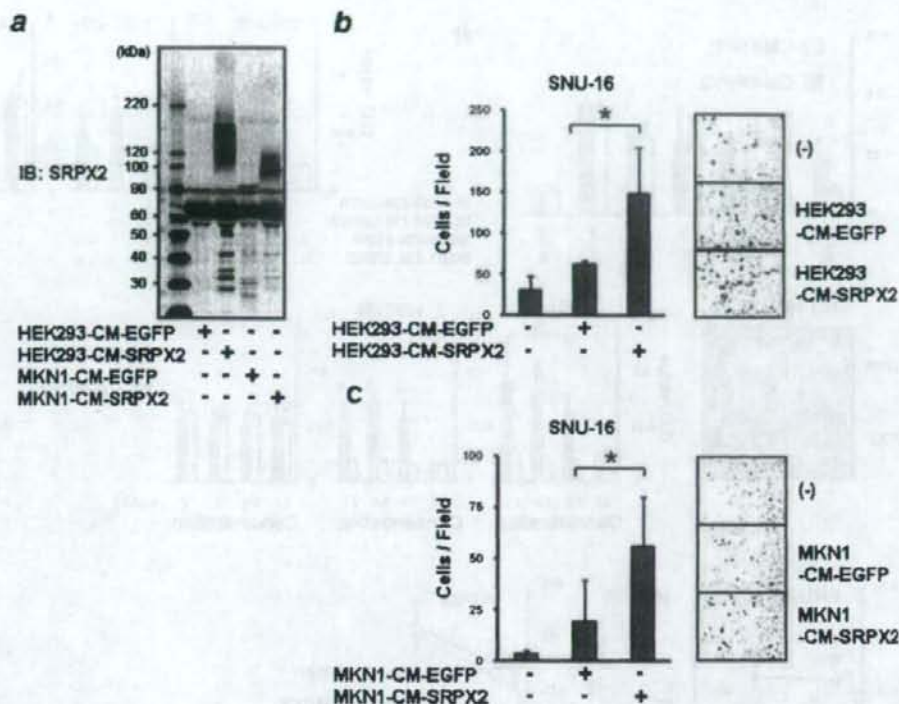
FIGURE 4 – SRPX2-conditioned medium enhanced cellular migration. (a) Western blotting for conditioned medium obtained from the stable cell lines, HEK293-pQCLIN-EGFP, HEK293-pQCLIN-SRPX2, MKN1-pQCLIN-EGFP and MKN1-pQCLIN-SRPX2. Each concentration of conditioned medium was adjusted to 1 mg/mL and diluted before use. Further details are described in the "Material and methods" section. IB, immunoblotting; HEK293-CM-EGFP, conditioned medium from HEK293-pQCLIN-EGFP cells; HEK293-CM-SRPX2, conditioned medium from HEK293-pQCLIN-SRPX2 cells; MKN1-CM-EGFP, conditioned medium from MKN1-pQCLIN-EGFP cells; MKN1-CM-SRPX2, conditioned medium from MKN1-pQCLIN-SRPX2 cells. The role of SRPX2 in cellular migration was assessed in the gastric cancer cell line, SNU-16, using a migration assay and EGFP- or SRPX2-conditioned medium from (b) HEK293-pQCLIN-EGFP or -SRPX2 cells and from (c) MKN1-pQCLIN-EGFP or -SRPX2 cells. A total of 1×10^5 SNU-16 cells were seeded into the upper chambers with 200 µL of RPMI containing 0.5% FBS. The final concentration of 100 µg/mL of EGFP-conditioned or SRPX2-conditioned medium was added to the 600 µL volume of the RPMI1640 containing 0.5% FBS medium in the lower chamber of the 24-well culture dish. The cells were incubated for 24 hr at 37°C. The number of migrated cells was evaluated as described earlier. The experiment was performed in triplicate. Representative data is shown in the right panels. The SRPX2-conditioned medium significantly enhanced cellular motility ($p < 0.05$) by about 2-fold, compared to the EGFP-conditioned medium. Data are shown as the mean ± SD of 3 independent experiments. *: $p < 0.05$.

cellular growth was seen between the cells, indicating that SRPX2 is not involved in cellular growth in HEK293 cells.

We next performed a migration assay to assess the role of SRPX2 in cellular motility. The cellular migration activity of the HEK293-pQCLIN-SRPX2 cells was significantly enhanced, compared to the EGFP transfectant cells ($p = 0.03$, Fig. 3b). A wound healing assay also demonstrated that the cellular motility of HEK293-pQCLIN-SRPX2 cells was significantly enhanced, compared to that of EGFP transfectant cells, at 8 and 12 hr after wound infliction ($p < 0.05$, Fig. 3c). Although the actual difference in the wound healing assay result was relatively small, these results indicate that SRPX2 is involved in cellular motility.

SRPX2-conditioned medium enhanced cellular migration

EGFP or SRPX2 was also introduced into a gastric cancer cell line, MKN1, and the SRPX2-conditioned media obtained from MKN1 and HEK293 cells were subjected to a migration assay. The transfected cells mainly produced the secreted type of SRPX2 protein with the higher molecular weight, as detected using western blot analysis. The SRPX2 proteins produced by MKN1 and western blot analysis. The SRPX2 proteins produced by MKN1 and

HEK293 cells were observed at ~95 kDa and 110–150 kDa, respectively (Fig. 4a). This difference in molecular weight might be due to glycosylation.

The role of the secreted SRPX2 protein in the conditioned medium on cellular migration was assessed to SNU-16 cells using a migration assay. SNU-16 cells were incubated for 24 hr in a normal culture medium containing 100 µg/mL of EGFP- or SRPX2-conditioned medium from HEK293-pQCLIN-EGFP or -SRPX2 cells added to the lower chamber of the 24-well culture dish. The SRPX2-conditioned medium significantly enhanced the cellular motility of the SNU-16 cells ($p < 0.05$) by about 2-fold higher than that of the EGFP-conditioned medium (Fig. 4b). Similar results were observed using conditioned medium from MKN1-pQCLIN-EGFP or -SRPX2 cells (Fig. 4c). This result indicates that the secreted SRPX2 protein increased cellular motility in gastric cancer cells.

SRPX2 protein promoted cellular attachment

We examined the cellular adhesion potential of 7 gastric cancer cell lines cultured on EGFP- and SRPX2-conditioned medium-
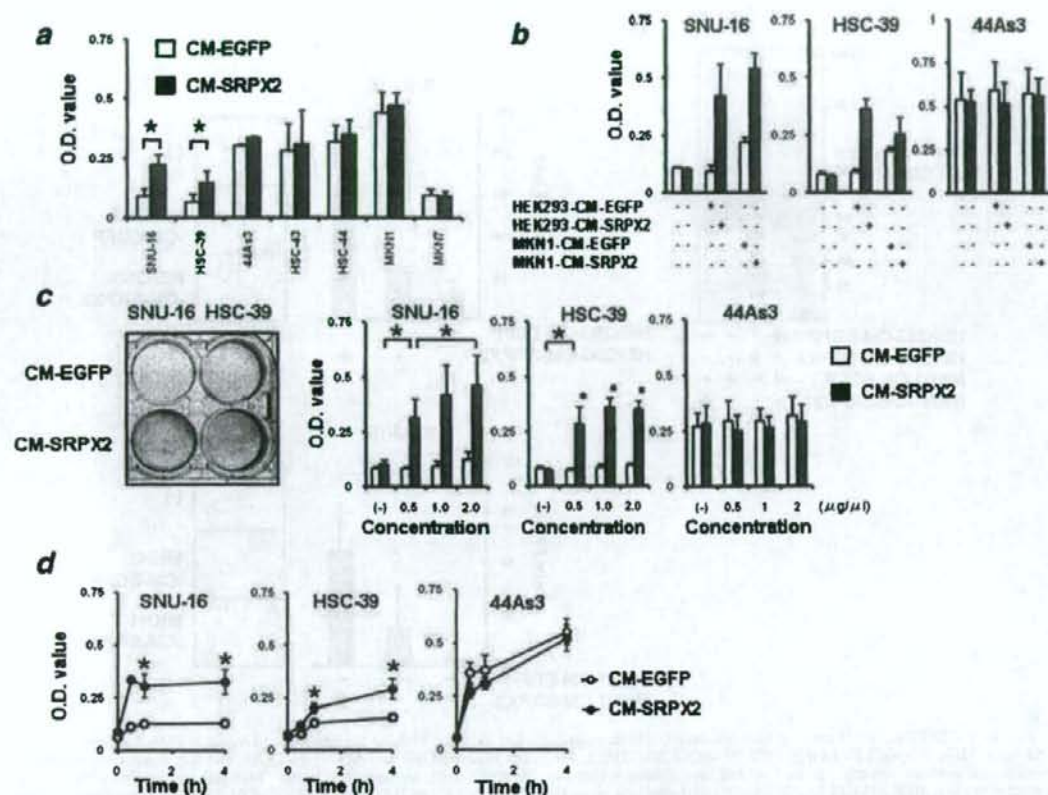
FIGURE 5 – SRPX2 protein enhanced cellular attachment. EGFP-conditioned or SRPX2-conditioned medium was adjusted to a concentration of 1 mg/mL and 50 µL was placed at 4°C overnight on 96-well plates. The conditioned medium was aspirated, and the wells were washed twice with phosphate-buffered saline (PBS). The plates were used in the adhesion assay as conditioned medium-coated 96-well plates. The cells to be analyzed (2×10^4 cells /well) were seeded into the wells of conditioned medium-coated plates and incubated at 37°C for 1 hr. The wells were then washed twice with PBS to remove nonadherent cells. The adherent cells were evaluated using an MTT assay. (a) A cellular adhesion assay was performed using 7 gastric cancer cell lines and conditioned medium-coated plates. The numbers of adhered SNU-16 and HSC-39 cells were significantly larger with the SRPX2-conditioned medium coated-plates ($p < 0.05$). (b) A cellular adhesion assay was also performed using conditioned medium-coated plates obtained from MKN1-pQCLIN-EGFP and MKN1-pQCLIN-SRPX2 cells. The numbers of adhered SNU-16 and HSC-39 cells, but not 44As3 cells, were significantly larger. (c) A cellular adhesion assay was performed using different concentrations of conditioned medium-coated plates. The 6-well-plate-scale data is shown in the left panel. (d) Cellular adhesion assay for time-course analysis. Larger numbers of attached SNU-16 and HSC-39 cells were observed from 0.5 to 4 hr. The increase in cellular attachment induced by the SRPX2 protein emerged after a relatively short time (0.5 hr). The experiment was performed in triplicate. CM-EGFP, conditioned medium from HEK293-pQCLIN-EGFP cells; CM-SRPX2, conditioned medium from HEK293-pQCLIN-SRPX2 cells. [Color figure can be viewed in the online issue, which is available at www.interscience.wiley.com.]

coated plates. Five of the gastric cancer cell lines did not increase cellular attachment to the conditioned medium-coated plate. However, the numbers of attached SNU-16 and HSC-39 cells were significantly increased by more than 2-fold by the presence of SRPX2 protein ($p < 0.05$, Fig. 5a).

To exclude nonspecific effects, cellular adhesion assays were also performed using conditioned medium-coated plates obtained from MKN1-pQCLIN-EGFP and MKN1-pQCLIN-SRPX2 cells (Fig. 5b). The SNU-16 and HSC-39 cells, but not the 44As3 cells, also exhibited a significantly larger number of adhered cells in the presence of SRPX2 protein obtained from the conditioned-medium of MKN1 cells. Cellular adhesion in these 3 cell lines was examined using 4 different concentrations of conditioned medium-coated plates. Similar results were obtained, and a dose-response effect for the conditioned medium was observed in SNU-16 cells (Fig. 5c). Time-course experiments revealed that a larger number of attached SNU-16 and HSC-39 cells were observed after

a short time (0.5 hr) to 4 hr after the start of incubation (Fig. 5d). Microscopic examination revealed that most of the adhered cells did not exhibit "cell spreading" and instead resembled "cellular attachment." These results demonstrate that SRPX2 is involved in cellular attachment in SNU-16 and HSC-39 cells.

SRPX2 protein increased phosphorylation levels of FAK

FAK plays a key role in cellular adhesion, and FAK signaling is considered to be a major pathway.[11] To gain insight into the function of SRPX2, the phosphorylation levels of FAK in SNU-16 cells were examined after culturing in a medium to which SRPX2-conditioned medium had been added. Increased phosphorylation levels of FAK (pY397 and pY576/577) were observed in SNU-16 cells in the presence of SRPX2, compared to EGFP, after 1–12 hr of culture (Fig. 6a). FAK phosphorylation occurred during an early stage (1 hr) and was consistent with the results for cellular
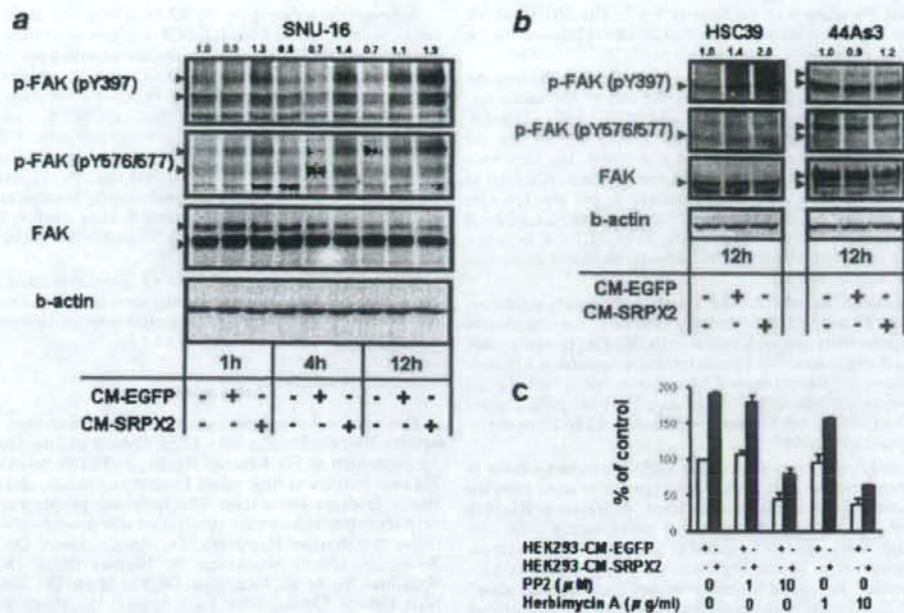
FIGURE 6 – SRPX2 protein increased the phosphorylation levels of FAK. The SNU-16 cells were cultured in RPMI with 0.5% FBS under the presence of GFP or SRPX2-conditioned medium at a final concentration of 100 μg /mL. The cells were collected at 1, 4 and 12 hr after incubation. Ten micrograms of cell lysate were subjected to western blotting using anti-phospho-FAK (pY397 and pY576/577), anti-FAK and anti-β-actin antibodies. A western blot was performed for (a) SNU-16 cells, and (b) HSC-39 and 44As3 cells. FAK, focal adhesion kinase; CM-EGFP, conditioned medium from HEK293-pQCLIN-EGFP cells; CM-SRPX2, conditioned medium from HEK293-pQCLIN-SRPX2 cells. Arrowheads: target molecules. The numerical densitometrical data of phospho-FAK (pY397) is shown above the western blot. (c) SNU-16 cells were treated with FAK inhibitors (PP2; final concentrations 1 or 10 μM and Herbimycin A; final concentrations 1 or 10 μg/mL) in a cellular adhesion assay to assess SRPX2-mediated attachment. Both PP2 and Herbimycin A inhibited cellular attachment of SNU-16 cells in dose-dependent manners. [Color figure can be viewed in the online issue, which is available at www.interscience.wiley.com.]

attachment. FAK phosphorylation by SRPX2 was also stimulated in HSC-39 cells but not in 44As3 cells (Fig. 6b). In addition, to determine whether FAK inhibitors could affect the SPRX2-mediated cellular attachment, the SNU-16 cells were treated with PP2[12] and Herbimycin A[13] to inhibit FAK activity in cellular adhesion assay (Fig. 6c). PP2 and Herbimycin A inhibited cellular attachment of SNU-16 cells in dose-dependent manners.

Although the molecules that transduce the extracellular SRPX2 signal into an intracellular signal remain unknown, these results suggest that the cellular phenotype caused by SRPX2 is associated with the FAK signaling pathway.

Discussion

Considering the structural features of *SRPX2*, the presence of both the sushi-repeat domain and the HYR domains predict an adhesive function.[4,5] We demonstrated that *SRPX2* enhanced cellular motility and cellular attachment, and these findings were consistent with the structural prediction.

The selectin family is the closest family to *SRPX2* and *SRPX*.[3] Selectins are known as cellular adhesion molecules and play key roles in the mediation of early neutrophil rolling on and adherence to endothelial cells.[14] Selectins recognize glycosylated proteins or lipids as their ligands, and this modification is necessary for their interaction.[15] The phylogenetical similarity between *SRPX2* and selectins suggests a similar biological function. SNU-16 and HSC-39 cells are basically nonadherent, and the increase in their cellular attachment was a relatively rapid response (0.5 hr). While number of attached cells increased significantly, the attachments

were weak and the cells did not spread on the plates. Thus, the increased cellular attachment induced by SRPX2 seems to resemble neutrophil rolling.

Because the DGEA motif is a potential integrin-binding motif[16] and this motif exists in the first sushi domain of SRPX2, we hypothesized that this motif is a critical binding site for SRPX2's ability to enhance cellular migration and attachment. We examined the inhibitory effect of the DGEA peptide[16] on cell migration and attachment, but no inhibitory effect was observed (data not shown). This result suggests that the cell migration and attachment induced by SRPX2 might be independent of DGEA sequence-mediated signal transduction, or such a sequon does not function in SRPX2.

FAK is a major focal adhesion-associated protein that transmits signals downstream of integrins. FAK signals control important biological events, including cell migration, proliferation and survival, through downstream molecules like Rho, Rac, Rap1, CDC42 and PAK.[11,17,18] Our results demonstrated that SRPX2 protein increased the phosphorylation levels of FAK in SNU-16 and HSC-39 cells, but not in 44As3 cells (Figs. 6a and 6b), and enhanced the cellular adhesive potential in SNU-16 and HSC-39 cells but not in 5 other cell lines (Fig. 5a). We speculate that certain molecules overexpressed in SNU-16 and HSC-39 cells may localize on the cell surface and bind to SRPX2 protein, activating FAK signaling. Recently, Royer-Zemmour *et al.*[19] demonstrated the interaction of SRPX2 with uPAR (plasminogen activator, urokinase receptor) as well as with other partners such as cathepsin B. Because uPAR particularly plays an important and well-known role in various tumoral processes including cell proliferation, migration, invasion and adhesion, and because uPAR-associated

intracellular signaling may act through FAK. The SRPX2/uPAR interaction might provide a possible molecular explanation for the role of SRPX2 in cancer.

Regarding the higher fuzzy smeared-band observed in only the culture medium (Figs. 2*b*, 2*c* and 4*a*), the size of the bands differed considerably between HEK293 and MKN1 cells (110–150 kDa and ~95 kDa, respectively). These results suggest that the higher smeared bands are probably not dimmers, but they may represent a highly glycosylated protein modification. We tried to cut off the N-glycans using N-glycosidase F, but the 150-kDa smeared band did not disappear. We plan to perform additional experiments to clarify the cause of the smeared band in future studies, the results of which will undoubtedly be useful in predicting the function of SRPX2.

Many studies have indicated that selectins, the family most similar to SRPX and SRPX2 proteins, increase the interaction between tumor cells and endothelial cells, leading to tumor progression and metastasis.[20,21] Thus selectins are considered promalignancy factors.[20] Recent reports have shown that selectins positively promote angiogenesis.[22,23] Because HUVEC cells express high levels of SRPX2 mRNA, the involvement of SRPX2 in angiogenesis should be clarified.

In this study, we demonstrated that SRPX2 is overexpressed in gastric cancer, compared to noncancerous gastric mucosa from the same patients, at the transcriptional level. A real-time RT-PCR analysis of 32 cell lines revealed that other cancer cells also express high levels of SRPX2 mRNA. SRPX2 was also overexpressed by more than 10-fold in clinical samples of colorectal cancers, compared to paired colonic mucosa (unpublished data). Thus, SRPX2 overexpression in cancer tissue may not be restricted to gastric cancers. We plan to further examine SRPX2 expression using immunohistochemistry in clinical samples of other cancers in the future.

Although the meaning of SRPX2 overexpression in gastric cancer is unclear, a real-time RT-PCR analysis of clinical samples showed that SRPX2 expression is associated with a poor prognosis in patients with gastric cancer. SRPX2 was first identified as a downstream molecule of E2F-HLF in pro-B acute leukemia with t(17;19) (q23;p13) and has since been reported to contribute to malignant phenotypes.[1] E2F-HLF-positive leukemia is characterized by a poor outcome with bone invasion, hypercalcemia and intravascular coagulation.[24] The clinical features of leukemia and our results for gastric cancer suggest that the biological function of SRPX2 is concerned with oncogenic activity. Further investigations of clinical outcome in relation to SRPX2 expression are needed.

In conclusion, we found that SRPX2 is overexpressed in gastric cancer and plays roles in cellular migration and adhesion in cancer cells. These results provide novel insight into the biological function of SRPX2 in cancer cells.

Acknowledgements

References

1. Kurosawa H, Goi K, Inukai T, Inaba T, Chang KS, Shinjyo T, Rakestraw KM, Naeve CW, Look AT. Two candidate downstream target genes for E2A-HLF. Blood 1999;93:321–32.
2. Roll P, Rudolf G, Pereira S, Royer B, Scheffer IE. Massacrier A, Valenti MP, Roeckel-Trevisiol N, Jamali S, Beclin C, Seegmuller C, Metz-Lutz MN, et al. SRPX2 mutations in disorders of language cortex and cognition. Hum Mol Genet 2006:15:1195–207.
3. Royer B, Soares DC, Barlow PN, Bontrop RE. Roll P, Robaglia-Schlupp A, Blancher A, Levasseur A, Cau P, Pontarotti P, Szepetowski P. Molecular evolution of the human SRPX2 gene that causes brain disorders of the Rolandic and Sylvian speech areas. BMC Genet 2007:8:72.
4. O'Leary JM, Bromek K, Black GM, Uhrinova S, Schmitz C, Wang X, Krych M, Atkinson JP, Uhrin D, Barlow PN. Backbone dynamics of complement control protein (CCP) modules reveals mobility in binding surfaces. Protein Sci 2004;13:1238–50.
5. Soares DC, Gerloff DL, Syme NR, Coulson AF, Parkinson J, Barlow PN. Large-scale modelling as a route to multiple surface comparisons of the CCP module family. Protein Eng Des Sel 2005;18:379–88.
6. Meindl A, Carvalho MR, Herrmann K, Lorenz B, Achatz H, Apfelstedt-Sylla E, Wittwer B, Ross M, Meitinger T, A gene (SRPX) encoding a sushi-repeat-containing protein is deleted in patients with X-linked retinitis pigmentosa. Hum Mol Genet 1995;4:2339–46.
7. Dry KL. Aldred MA, Edgar AJ, Brown J. Manson FD, Ho MF. Prosser J, Hardwick LJ, Lennon AA, Thomson K, Keuren MV, Kumit DM, et al. Identification of a novel gene, ETX1 from Xp21.1, a candidate gene for X-linked retintis pigmentosa (RP3). Hum Mol Genet 1995;4:2347–53.
8. Callebaut I, Gilges D, Vigon I, Mornon JP. HYR, an extracellular module involved in cellular adhesion and related to the immunoglobulin-like fold. Protein Sci 2000;9:1382–90.
9. Yamada Y, Arao T, Gotoda T, Taniguchi H, Oda I, Shirao K, Shimada Y, Hamaguchi T, Kato K, Hamano T, Koizumi F, Tamura T, et al. Identification of prognostic biomarkers in gastric cancer using endoscopic biopsy samples. Cancer Sci 2008;99:2193–99.
10. Yamanaka R, Arao T, Yajima N, Tsuchiya N, Homma J, Tanaka R, Sano M, Oide A, Sekijima M, Nishio K. Identification of expressed genes characterizing long-term survival in malignant glioma patients. Oncogene 2006;25:5994–6002.
11. Parsons JT. Focal adhesion kinase: the first ten years. J Cell Sci 2003; 116:1409–16.
12. Pala D, Kapoor M, Woods A, Kennedy L, Liu S, Chen S, Bursell L, Lyons KM, Carter DE, Beier F, Leask A. Focal adhesion kinase/Src suppresses early chondrogenesis: central role of CCN2. J Biol Chem 2008;283:9239–47.
13. Lan CC, Wu CS, Chiou MH, Hsieh PC, Yu HS. Low-energy heliumneon laser induces locomotion of the immature melanoblasts and promotes melanogenesis of the more differentiated melanoblasts: recapitulation of vitiligo repigmentation in vitro. J Invest Dermatol 2006; 126:2119–26.
14. Mousa SA. Cell adhesion molecules: potential therapeutic & diagnostic implications. Mol Biotechnol 2008;38:33–40.
15. Vestweber D, Blanks JE. Mechanisms that regulate the function of the selectins and their ligands. Physiol Rev 1999;79:181–213.
16. Mineur P, Guignandon A. Lambert ChA, Amblard M, Lapiere ChM, Nusgens BV. RGDS and DGEA-induced [Ca2+]i signalling in human dermal fibroblasts. Biochim Biophys Acta 2005;1746:28–37.
17. Schaller MD. FAK and paxillin: regulators of N-cadherin adhesion and inhibitors of cell migration? J Cell Biol 2004;166:157–9.
18. Mitra SK, Schlaepfer DD. Integrin-regulated FAK-Src signaling in normal and cancer cells. Curr Opin Cell Biol 2006;18:516–23.
19. Royer-Zemmour B, Ponsole-Lenfant M, Gara H, Roll P, Leveque C, Massacrier A, Ferracci G, Cillario J, Robaglia-Schlupp A, Vincentelli R, Cau P, Szepetowski P. Epileptic and developmental disorders of the speech cortex: ligand/receptor interaction of wild-type and mutant SRPX2 with the plasminogen activator receptor uPAR. Hum Mol Genet 2008;17:3617–30.
20. Witz IP. The selectin-selectin ligand axis in tumor progression. Cancer Metastasis Rev 2008;27:19–30.
21. Barthel SR, Gavino JD, Descheny L, Dimitroff CJ. Targeting selectins and selectin ligands in inflammation and cancer. Expert Opin Ther Targets 2007;11:1473–91.
22. Oh IY, Yoon CH, Hur J, Kim JH, Kim TY, Lee CS, Park KW, Chae IH, Oh BH. Park YB, Kim HS. Involvement of E-selectin in recruitment of endothelial progenitor cells and angiogenesis in ischemic muscle. Blood 2007;110:3891–9.
23. Egami K, Muroharu T, Aoki M, Matsuishi T. Ischemia-induced angiogenesis: role of inflammatory response mediated by P-selectin. J Leukoc Biol 2006;79:971–6.
24. Hunger SP. Chromosomal translocations involving the E2A gene in acute lymphoblastic leukemia: clinical features and molecular pathogenesis. Blood 1996;87:1211–24.

The anti-EGFR monoclonal antibody blocks cisplatin-induced activation of EGFR signaling mediated by HB-EGF

Takeshi Yoshida[a], Isamu Okamoto[a,*], Tsutomu Iwasa[a], Masahiro Fukuoka[b], Kazuhiko Nakagawa[a]

[a] Department of Medical Oncology, Kinki University School of Medicine, 377-2 Ohno-higashi, Osaka-Sayama, Osaka 589-8511, Japan
[b] Kinki University School of Medicine, Sakai Hospital, 2-7-1 Harayamadai, Minami-ku Sakai, Osaka 590-0132, Japan

Abstract Cisplatin is a key agent in combination chemotherapy for various types of solid tumor. We now show that cisplatin activates signaling by the epidermal growth factor receptor (EGFR) by inducing cleavage of heparin-binding epidermal growth factor-like growth factor (HB-EGF). Matuzumab, a monoclonal antibody to EGFR, inhibited cisplatin-induced EGFR signaling, likely through competition with the soluble form of HB-EGF for binding to EGFR. Matuzumab enhanced the antitumor effect of cisplatin in nude mice harboring human non-small cell lung cancer xenografts. Our findings shed light on the mechanism by which monoclonal antibodies to EGFR might augment the efficacy of cisplatin.

Crown Copyright © 2008 Published by Elsevier B.V. on behalf of the Federation of European Biochemical Societies. All rights reserved.

Keywords: EGF receptor; Heparin-binding EGF-like growth factor; Matuzumab; Cisplatin; Non-small cell lung cancer

1. Introduction

Cisplatin is a key component of combination chemotherapy for various types of solid tumor, but its effectiveness is limited by the development of chemoresistance [1]. Several nonphysiological stimuli that induce cellular stress, such as hyperosmolarity, wounding, UV or γ-radiation, reactive oxygen species, and chemotherapeutic agents, trigger activation of the epidermal growth factor receptor (EGFR) [2–11]. Ligand binding to EGFR induces receptor dimerization and activation of the receptor kinase, triggering intracellular signaling pathways such as those mediated by the protein kinases Akt or extracellular signal-regulated kinase (Erk), which play fundamental roles in the control of numerous cellular processes such as growth, proliferation, and survival [12–18]. EGFR signaling pathways activated by cellular stressors are thus of clinical interest because of their potential role in tumor resistance to chemotherapy [2–11]. The effects of cisplatin on EGFR signaling pathways have remained unclear, but the potential role of

these pathways in cisplatin resistance makes it important to examine whether EGFR inhibitors might enhance the antitumor effects of this drug [8,9].

We have now examined the molecular mechanism of cisplatin-induced activation of EGFR and the effects of this drug on downstream signaling pathways. We also examined the effects of matuzumab (EMD72000, humanized mouse immunoglobulin G1), a monoclonal antibody (mAb) to EGFR [19], on cisplatin-dependent EGFR signaling. Finally, the antitumor effect of matuzumab combined with cisplatin was evaluated in order to provide insight into the mechanism by which anti-EGFR mAbs might augment the efficacy of cisplatin.

2. Materials and methods

2.1. Cell culture and reagents

The human non-small cell lung cancer (NSCLC) cell lines NCI-H292 (H292), NCI-H460 (H460), and A549 were obtained and cultured as previously described [20]. Matuzumab and gefitinib were also obtained as previously described [19]; GM6001 was from Calbiochem (La Jolla, CA); cisplatin, CRM197, and epidermal growth factor (EGF) were from Sigma (St. Louis, MO); and heparin-binding EGF-like growth factor (HB-EGF) was from R&D Systems (Minneapolis, MN).

2.2. Immunoblot analysis

Immunoblot analysis was performed as described previously [20]. Primary antibodies to the Tyr[845]-phosphorylated form of EGFR, to EGFR, to phosphorylated Erk, to Erk, to phosphorylated Akt, and to Akt as well as horseradish peroxidase (HRP)-conjugated goat antibodies to mouse or rabbit immunoglobulin G were obtained as described previously [20]. Primary antibodies to the intracellular COOH-terminal domain of HB-EGF and HRP-conjugated donkey antibodies to goat immunoglobulin G were from Santa Cruz Biotechnology (Santa Cruz, CA).

2.3. Assessment of tumor growth inhibition in vivo

Tumor cells (2×10^6) were injected subcutaneously into the flank of 7-week-old female athymic nude mice. The mice were divided into four treatment groups of seven or eight animals: those treated over 2 weeks by intraperitoneal injection of vehicle, matuzumab (0.05 mg, twice per week), cisplatin (6 mg/kg of body weight, twice per week), or both matuzumab and cisplatin. Treatment was initiated when tumors in each group achieved an average volume of 200 mm^3, with tumor volume being determined twice weekly for 41 days after the onset of treatment from caliper measurement of tumor length (L) and width (W) according to the formula $LW^2/2$.

2.4. Ki67 index

Tumors were removed from some animals 14 days after treatment initiation and were stained with a mouse mAb to human Ki67 (clone MIB-1; Dako, Carpinteria, CA), as previously described [21]. The

*Corresponding author. Fax: +81 72 360 5000.
E-mail address: chi-okamoto@dotd.med.kindai.ac.jp (I. Okamoto).

Abbreviations: EGF, epidermal growth factor; EGFR, EGF receptor; mAb, monoclonal antibody; NSCLC, non-small cell lung cancer; HB-EGF, heparin-binding EGF-like growth factor; HRP, horseradish peroxidase; TUNEL, terminal deoxynucleotidyl transferase-mediated dUTP nick-end labeling

Ki67 index was determined as the percentage of Ki67-positive cells by scoring at least 300 tumor cells in each of 10 well-preserved fields of each tumor at a magnification of ×200 (CX41 light microscope; Olympus, Tokyo, Japan).

2.5. TUNEL staining

Terminal deoxynucleotidyl transferase-mediated dUTP nick-end labeling (TUNEL) analysis of tumor sections was performed as de-

scribed previously [22]. The number of apoptotic cells in each of 10 fields (×200) per tumor was determined with a light microscope (CX41, Olympus).

2.6. Statistical analysis

Quantitative data are presented as means ± S.D. and were compared among groups by one-way analysis of variance followed by Tukey's multiple comparison test. A P value of <0.05 was considered
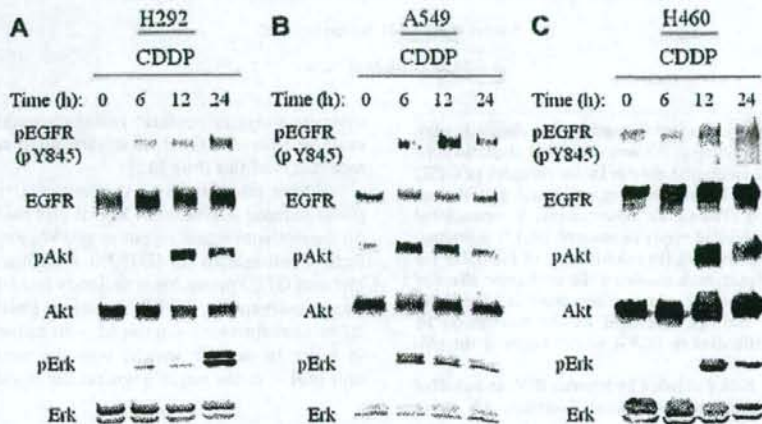

Fig. 1. Cisplatin-induced activation of EGFR and of downstream signaling pathways mediated by Akt or Erk. Serum-deprived H292 (A), A549 (B), or H460 (C) cells were incubated for the indicated times in the absence or presence of cisplatin (CDDP, 100 μM). Cell lysates were then subjected to immunoblot analysis with antibodies to the Tyr[845]-phosphorylated form of EGFR (pEGFR), to phosphorylated Akt, or to phosphorylated Erk as well as with antibodies to total forms of these proteins.
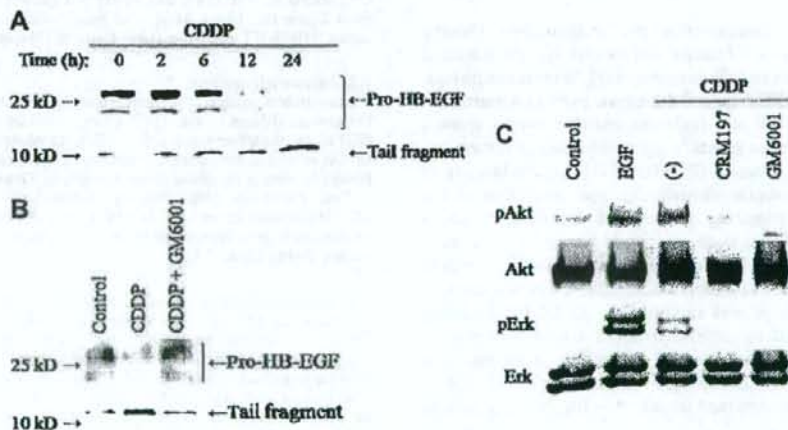

Fig. 2. Cisplatin-induced HB-EGF cleavage and its role in activation of EGFR signaling pathways by cisplatin. (A) Serum-deprived H292 cells were incubated for the indicated times in the presence of cisplatin (100 μM). Cell lysates were then subjected to immunoblot analysis with antibodies to the intracellular COOH-terminal domain of HB-EGF. The positions of molecular size standards (left) as well as of bands corresponding to pro-HB-EGF and to the cleaved tail fragment (right) are indicated. (B) Serum-deprived H292 cells were incubated alone (control) or with cisplatin (100 μM) in the absence or presence of GM6001 (10 μM) for 12 h. Cell lysates were then subjected to immunoblot analysis as in (A). (C) Serum-deprived H292 cells were incubated with EGF (100 ng/ml) for 15 min as a positive control or with cisplatin (100 μM) in the absence or presence of GM6001 (10 μM) or CRM197 (10 μg/ml) for 12 h. Cell lysates were then subjected to immunoblot analysis with antibodies to phosphorylated or total forms of Akt or Erk.

statistically significant. Statistical analysis was performed with Graph-Pad Prism version 5.00 for Windows (GraphPad Software, San Diego, CA).

3. Results and discussion

3.1. Cisplatin activates EGFR as well as downstream Akt and Erk signaling pathways

Cellular stress induced by several chemotherapeutic agents or γ-radiation triggers the activation of EGFR signaling pathways, with this effect being thought to play an important role in resistance to chemotherapy or radiotherapy [6–11]. We examined the effects of cisplatin on EGFR and downstream signaling pathways mediated by Akt or Erk in human NSCLC cell lines (H292, A549. H460). Cisplatin induced the phosphorylation of EGFR, Akt, and Erk in a time-dependent manner, without affecting the total amounts of these proteins, in all three cell lines (Fig. 1). These results thus showed that cisplatin

activates EGFR and downstream signaling pathways mediated by Akt or Erk.

3.2. Cisplatin activates EGFR signaling pathways by inducing the cleavage of HB-EGF

HB-EGF is a membrane-bound EGFR ligand that activates EGFR after its release from the membrane in response to cellular stress [3,5,23–25]. To determine whether HB-EGF contributes to cisplatin-induced EGFR signaling, we examined the possible effect of cisplatin on cleavage of the membrane-bound pro-form of HB-EGF in H292 cells. Cisplatin induced a time-dependent decrease in the amount of pro-HB-EGF and a consequent increase in the amount of a COOH-terminal fragment of this protein referred to as the "tail fragment" (Fig. 2A). These effects of cisplatin were inhibited by GM6001 (Fig. 2B), a potent inhibitor of matrix metalloproteinases responsible for HB-EGF cleavage [23,24], suggesting that cisplatin induces metalloproteinase-mediated cleavage of the ectodomain of HB-EGF and its release from the cell sur-
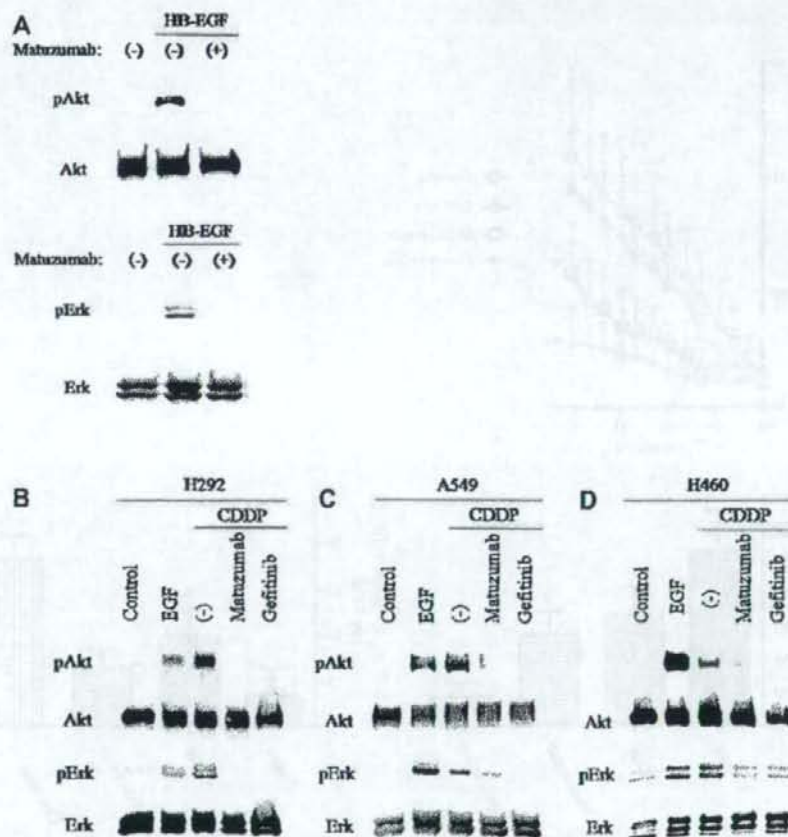

Fig. 3. Inhibition by matuzumab of EGFR signaling induced by HB-EGF or by cisplatin. (A) Serum-deprived H292 cells were incubated first for 2 h in the absence or presence of matuzumab (200 nM) and then for 15 min in the additional absence or presence of HB-EGF (10 ng/ml). Cell lysates were then subjected to immunoblot analysis with antibodies to phosphorylated or total forms of Akt or Erk. (B–D) Serum-deprived H292 (B), A549 (C), or H460 (D) cells were incubated with EGF (100 ng/ml) for 15 min as a positive control or with cisplatin (100 μM) in the absence or presence of matuzumab (200 nM) or gefitinib (10 μM) for 12 h. Cell lysates were then subjected to immunoblot analysis as in (A).

face. GM6001 also blocked the activation of Akt and Erk by cisplatin (Fig. 2C), implicating HB-EGF cleavage in cisplatin-induced EGFR signaling. To explore further whether cisplatin-induced EGFR signaling is dependent on HB-EGF activity, we examined the effect of CRM197, a nontoxic mutant form of diphtheria toxin that binds specifically to and neutralizes HB-EGF, which has also been identified as a diphtheria toxin receptor [26]. CRM197 completely inhibited the activation of Akt and Erk by cisplatin (Fig. 2C), suggesting that cisplatin promotes EGFR signaling by inducing the cleavage of HB-EGF. Consistent with this notion, the time course of cisplatin-induced activation of EGFR signaling (Fig. 1A) was similar to that of cisplatin-induced release of HB-EGF from the cell surface (Fig. 2A).

Cisplatin has previously been shown to increase the amount of HB-EGF mRNA in various types of cancer cells [7], and expression of the HB-EGF gene was found to be increased in cisplatin-resistant cancer [27]. The chemotherapeutic drugs SN38, doxorubicin, and imatinib also induce EGFR signaling and subsequent chemoresistance through metalloproteinase-dependent cleavage of HB-EGF [7,10]. It is possible that EGFR signaling resulting from metalloproteinase-mediated cleavage of HB-EGF represents a common mechanism of cellular resistance to various chemotherapeutic agents.

3.3. Effects of matuzumab on cisplatin-induced EGFR signaling

The clinical efficacy of treatment with anti-EGFR mAbs has been thought to be due to their prevention of ligand binding to EGFR [28,29]. We hypothesized that anti-EGFR mAbs might inhibit cisplatin-induced EGFR signaling by blocking the binding of the released ectodomain of HB-EGF to EGFR. To test whether anti-EGFR mAbs inhibit EGFR signaling induced by HB-EGF, we examined the effects of the humanized anti-EGFR mAb matuzumab. Matuzumab indeed prevented the activation of Akt and Erk by HB-EGF (Fig. 3A), indicating that this mAb inhibits HB-EGF–dependent EGFR signaling. We next examined the effect of matuzumab on cisplatin-induced EGFR signal transduction. The activation of EGFR downstream signaling by cisplatin was abolished by gefitinib in H292, A549, and H460 cells (Fig. 3B–D), suggesting that cisplatin-induced EGFR signaling requires the tyrosine kinase activity of EGFR. Matuzumab also markedly inhibited
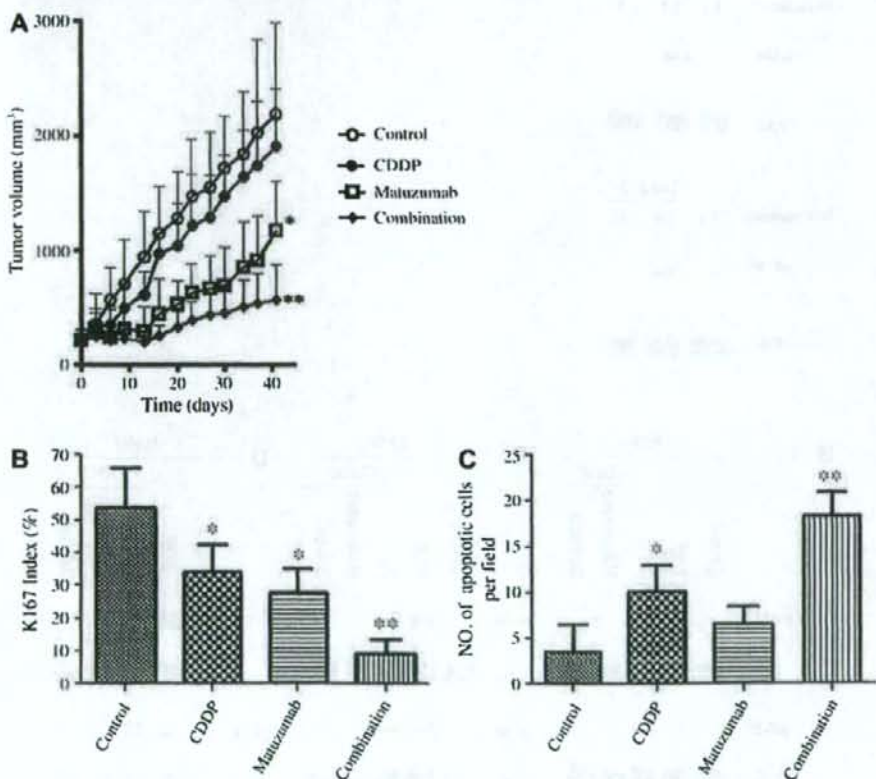

Fig. 4. Enhancement by matuzumab of the antitumor effect of cisplatin in vivo. (A) Nude mice harboring H292 tumor xenografts (200 mm³) were treated with a single intraperitoneal dose of matuzumab (0.05 mg) or cisplatin (6 mg/kg), with both agents, or with vehicle (control) twice a week for 14 days. Tumor volume was determined at the indicated times after the onset of treatment. (B) The Ki67 index was determined from sections of H292 tumor xenografts 14 days after the initiation of treatment as in (A). (C) Quantitation by TUNEL staining of the number of apoptotic cells per field (×200) in H292 tumor xenografts 14 days after the initiation of treatment as in (A). Data in (A–C) are means ± S.D. *P < 0.05 versus control; **P < 0.05 versus control or each agent alone.

cisplatin-induced EGFR signaling in all three cell lines (Fig. 3B–D). These results thus suggested that matuzumab blocks cisplatin-induced EGFR signaling through inhibition of HB-EGF-dependent activation of EGFR.

Matuzumab exerts its antitumor effect both by competition with EGF for binding to EGFR and by blockade of the EGFR turnover that is important for activation of downstream signaling pathways mediated by Akt or Erk [19,28,29]. The soluble form of HB-EGF includes the EGF-like domain, a common structure in members of the EGF family of proteins that consists of 40–45 amino acids and contains six cysteine residues, but it binds not only to EGFR but also to ErbB4, whereas EGF binds specifically to EGFR [23–25]. The corresponding binding site of EGFR or the ligand function of HB-EGF may therefore differ from those for EGF. Nevertheless, we have now shown that matuzumab also inhibits the activation of EGFR signaling by both HB-EGF and cisplatin.

3.4. Matuzumab enhances the antitumor action of cisplatin in H292 xenografts

If cisplatin-induced EGFR signaling plays an important role in the development of cisplatin resistance, matuzumab might be expected to enhance the antitumor effect of cisplatin by inhibiting such signaling. We therefore determined the efficacy of combined treatment with matuzumab and cisplatin in nude mice with solid tumors formed by H292 cells injected into the flank. Combination therapy with matuzumab and cisplatin inhibited tumor growth to a significantly greater extent than did treatment with matuzumab or cisplatin alone (Fig. 4A).

Tumors treated with the combination of matuzumab and cisplatin also manifested both a significantly smaller Ki67 index (Fig. 4B), a marker of cell proliferation, and a significantly greater proportion of apoptotic cells (Fig. 4C), compared with tumors treated with either agent alone. Matuzumab alone or in combination with cytotoxic agents was previously shown to inhibit Akt or Erk phosphorylation in human tissue samples or human xenografts in nude mice [30–34]. The combination of matuzumab and cisplatin likely reduced the Ki67 index in the present study because matuzumab blocked the cisplatin-induced activation of Erk, which is important for cancer cell proliferation as a component of the Ras-MEK-Erk signaling pathway [17,18]. The increase in the number of apoptotic cells in tumors treated with both matuzumab and cisplatin likely resulted from inhibition by matuzumab of the cisplatin-induced activation of Akt, which contributes to antiapoptotic signaling through several pathways [15,16]. Our data thus indicate that matuzumab enhanced the antitumor effect of cisplatin, with the combination treatment inhibiting tumor cell proliferation and inducing apoptosis to a greater extent than treatment with either agent alone. Our data showing that gefitinib also blocked cisplatin-induced activation of Akt and Erk may explain the previous observation that the growth-inhibitory action of cisplatin in A549 tumors was increased fourfold in combination with gefitinib [35]. Our findings suggest the importance of EGFR signaling in the development of chemoresistance to cisplatin, and they provide insight into the mechanism by which anti-EGFR mAbs might augment the efficacy of cisplatin. Clinical studies of the therapeutic efficacy of matuzumab combined with cisplatin are thus warranted.

References

[1] Siddik, Z.H. (2003) Cisplatin: mode of cytotoxic action and molecular basis of resistance. Oncogene 22, 7265–7279.

[2] El-Abaseri, T.B., Putta, S. and Hansen, L.A. (2006) Ultraviolet irradiation induces keratinocyte proliferation and epidermal hyperplasia through the activation of the epidermal growth factor receptor. Carcinogenesis 27, 225–231.

[3] Xu, K.P., Ding, Y., Ling, J., Dong, Z. and Yu, F.S. (2004) Wound-induced HB-EGF ectodomain shedding and EGFR activation in corneal epithelial cells. Invest. Ophthalmol. Vis. Sci. 45, 813–820.

[4] King, C.R., Borrello, I., Porter, L., Comoglio, P. and Schlessinger, J. (1989) Ligand-independent tyrosine phosphorylation of EGF receptor and the erbB-2/neu proto-oncogene product is induced by hyperosmotic shock. Oncogene 4, 13–18.

[5] Chen, C.H., Cheng, T.H., Lin, H., Shih, N.L., Chen, Y.L., Chen, Y.S., Cheng, C.F., Lian, W.S., Meng, T.C., Chiu, W.T. and Chen, J.J. (2006) Reactive oxygen species generation is involved in epidermal growth factor receptor transactivation through the transient oxidization of Src homology 2-containing tyrosine phosphatase in endothelin-1 signaling pathway in rat cardiac fibroblasts. Mol. Pharmacol. 69, 1347–1355.

[6] Park, C.M., Park, M.J., Kwak, H.J., Lee, H.C., Kim, M.S., Lee, S.H., Park, I.C., Rhee, C.H. and Hong, S.I. (2006) Ionizing radiation enhances matrix metalloproteinase-2 secretion and invasion of glioma cells through Src/epidermal growth factor receptor-mediated p38/Akt and phosphatidylinositol 3-kinase/Akt signaling pathways. Cancer Res. 66, 8511–8519.

[7] Wang, F., Liu, R., Lee, S.W., Sloss, C.M., Couper, J. and Cusack, J.C. (2007) Heparin-binding EGF-like growth factor is an early response gene to chemotherapy and contributes to chemotherapy resistance. Oncogene 26, 2006–2016.

[8] Winograd-Katz, S.E. and Levitzki, A. (2006) Cisplatin induces PKB/Akt activation and p38(MAPK) phosphorylation of the EGF receptor. Oncogene 25, 7381–7390.

[9] Benhar, M., Engelberg, D. and Levitzki, A. (2002) Cisplatin-induced activation of the EGF receptor. Oncogene 21, 8723–8731.

[10] Johnson, F.M., Saigal, B. and Donato, N.J. (2005) Induction of heparin-binding EGF-like growth factor and activation of EGF receptor in imatinib mesylate-treated squamous carcinoma cells. J. Cell. Physiol. 205, 218–227.

[11] Van Schaeybroeck, S., Kyula, J., Kelly, D.M., Karaiskou-McCaul, A., Stokesberry, S.A., Van Cutsem, E., Longley, D.B. and Johnston, P.G. (2006) Chemotherapy-induced epidermal growth factor receptor activation determines response to combined gefitinib/chemotherapy treatment in non-small cell lung cancer cells. Mol. Cancer Ther. 5, 1154–1165.

[12] Carpenter, G. (1987) Receptors for epidermal growth factor and other polypeptide mitogens. Annu. Rev. Biochem. 56, 881–914.

[13] Klapper, L.N., Kirschbaum, M.H., Sela, M. and Yarden, Y. (2000) Biochemical and clinical implications of the ErbB/HER signaling network of growth factor receptors. Adv. Cancer Res. 77, 25–79.

[14] Di Marco, E., Pierce, J.H., Fleming, T.P., Kraus, M.H., Molloy, C.J., Aaronson, S.A. and Di Fiore, P.P. (1989) Autocrine interaction between TGFα and the EGF-receptor: quantitative requirements for induction of the malignant phenotype. Oncogene 4, 831–838.

[15] Datta, S.R., Brunet, A. and Greenberg, M.E. (1999) Cellular survival: a play in three Akts. Genes Dev. 13, 2905–2927.

[16] Goswami, A., Ranganathan, P. and Rangnekar, V.M. (2006) The phosphoinositide 3-kinase/Akt1/Par-4 axis: a cancer-selective therapeutic target. Cancer Res. 66, 2889–2892.

[17] Katz, M., Amit, I. and Yarden, Y. (2007) Regulation of MAPKs by growth factors and receptor tyrosine kinases. Biochim. Biophys. Acta 1773, 1161–1176.

[18] Roberts, P.J. and Der, C.J. (2007) Targeting the Raf-MEK-ERK mitogen-activated protein kinase cascade for the treatment of cancer. Oncogene 26, 3291–3310.

[19] Yoshida, T., Okamoto, I., Okabe, T., Iwasa, T., Satoh, T., Nishio, K., Fukuoka, M. and Nakagawa, K. (2008) Matuzumab and cetuximab activate the epidermal growth factor receptor but fail to trigger downstream signaling by Akt or Erk. Int. J. Cancer 122, 1530–1538.

[20] Okabe, T., Okamoto, I., Tamura, K., Terashima, M., Yoshida, T., Satoh, T., Takada, M., Fukuoka, M. and Nakagawa, K. (2007) Differential constitutive activation of the epidermal growth factor receptor in non-small cell lung cancer cells bearing EGFR gene mutation and amplification. Cancer Res. 67, 2046–2053.

[21] Wu, L., Birle, D.C. and Tannock, I.F. (2005) Effects of the mammalian target of rapamycin inhibitor CCI-779 used alone or with chemotherapy on human prostate cancer cells and xenografts. Cancer Res. 65, 2825–2831.

[22] Akashi, Y., Okamoto, I., Iwasa, T., Yoshida, T., Suzuki, M., Hatashita, E., Yamada, Y., Satoh, T., Fukuoka, M., Ono, K. and Nakagawa, K. (2007) The novel microtubule-interfering agent TZT-1027 enhances the anticancer effect of radiation in vitro and in vivo. Br. J. Cancer 96, 1532–1539.

[23] Higashiyama, S. and Nanba, D. (2005) ADAM-mediated ectodomain shedding of HB-EGF in receptor cross-talk. Biochim. Biophys. Acta 1751, 110–117.

[24] Miyamoto, S., Yagi, H., Yotsumoto, F., Kawarabayashi, T. and Mekada, E. (2006) Heparin-binding epidermal growth factor-like growth factor as a novel targeting molecule for cancer therapy. Cancer Sci. 97, 341–347.

[25] Ono, M., Raab, G., Lau, K., Abraham, J.A. and Klagsbrun, M. (1994) Purification and characterization of transmembrane forms of heparin-binding EGF-like growth factor. J. Biol. Chem. 269, 31315–31321.

[26] Mitamura, T., Higashiyama, S., Taniguchi, N., Klagsbrun, M. and Mekada, E. (1995) Diphtheria toxin binds to the epidermal growth factor (EGF)-like domain of human heparin-binding EGF-like growth factor/diphtheria toxin receptor and inhibits specifically its mitogenic activity. J. Biol. Chem. 270, 1015–1019.

[27] Suganuma, K., Kubota, T., Saikawa, Y., Abe, S., Otani, Y., Furukawa, T., Kumai, K., Hasegawa, H., Watanabe, M., Kitajima, M., Nakayama, H. and Okabe, H. (2003) Possible chemoresistance-related genes for gastric cancer detected by cDNA microarray. Cancer Sci. 94, 355–359.

[28] Li, S., Schmitz, K.R., Jeffrey, P.D., Wiltzius, J.J., Kussie, P. and Ferguson, K.M. (2005) Structural basis for inhibition of the epidermal growth factor receptor by cetuximab. Cancer Cell 7, 301–311.

[29] Adams, G.P. and Weiner, L.M. (2005) Monoclonal antibody therapy of cancer. Nat. Biotechnol. 23, 1147–1157.

[30] Kleespies, A., Ischenko, I., Eichhorn, M.E., Seeliger, H., Amendt, C., Mantell, O., Jauch, K.W. and Bruns, C.J. (2008) Matuzumab short-term therapy in experimental pancreatic cancer: prolonged antitumor activity in combination with gemcitabine. Clin. Cancer Res. 14, 5426–5436.

[31] Graeven, U., Kremer, B., Sudhoff, T., Killing, B., Rojo, F., Weber, D., Tillner, J., Unal, C. and Schmiegel, W. (2006) Phase I study of the humanised anti-EGFR monoclonal antibody matuzumab (EMD 72000) combined with gemcitabine in advanced pancreatic cancer. Br. J. Cancer 94, 1293–1299.

[32] Rao, S., Starling, N., Cunningham, D., Benson, M., Wotherspoon, A., Lupfert, C., Kurek, R., Oates, J., Baselga, J. and Hill, A. (2008) Phase I study of epirubicin, cisplatin and capecitabine plus matuzumab in previously untreated patients with advanced oesophagogastric cancer. Br. J. Cancer 99, 868–874.

[33] Vanhoefer, U., Tewes, M., Rojo, F., Dirsch, O., Schleucher, N., Rosen, O., Tillner, J., Kovar, A., Braun, A.H., Trarbach, T., Seeber, S., Harstrick, A. and Baselga, J. (2004) Phase I study of the humanized antiepidermal growth factor receptor monoclonal antibody EMD72000 in patients with advanced solid tumors that express the epidermal growth factor receptor. J. Clin. Oncol. 22, 175–184.

[34] Salazar, R., Tabernero, J., Rojo, F., Jimenez, E., Montaner, I., Casado, E., Sala, G., Tillner, J., Malik, R. and Baselga, J. (2004) Dose-dependent inhibition of the EGFR and signalling pathways with the anti-EGFR monoclonal antibody (MAb) EMD 72000 administered every three weeks (q3w). A phase I pharmacokinetic/pharmacodynamic (PK/PD) study to define the optimal biological dose (OBD). J. Clin. Oncol. 22 (Suppl. 14), 127.

[35] Sirotnak, F.M., Zakowski, M.F., Miller, V.A., Scher, H.I. and Kris, M.G. (2000) Efficacy of cytotoxic agents against human tumor xenografts is markedly enhanced by coadministration of ZD1839 (Iressa), an inhibitor of EGFR tyrosine kinase. Clin. Cancer Res. 6, 4885–4892.

Case Report

Therapy-Related Acute Promyelocytic Leukemia Caused by Hormonal Therapy and Radiation in a Patient with Recurrent Breast Cancer

Makiko Ono[1], Takashi Watanabe[2], Chikako Shimizu[1], Nobuhiro Hiramoto[2], Yasushi Goto[2], Kan Yonemori[1], Tsutomu Kouno[1], Masashi Ando[1], Kenji Tamura[1], Noriyuki Katsumata[1] and Yasuhiro Fujiwara[1]

[1]Breast and Medical Oncology Division and [2]Hematology Division, National Cancer Center Hospital, Tokyo, Japan

We report a patient with therapy-related acute promyelocytic leukemia (APL) that may have been caused by regional radiation or hormonal therapy after surgery. A 36-year-old Japanese woman developed right breast cancer and underwent breast-conserving surgery and regional radiation to the right breast without adjuvant systemic therapy because she wished to preserve her fertility. Two years later, she developed multiple bone metastases of breast cancer and received hormonal therapy. During the second line hormonal therapy, she developed APL and received induction and consolidation chemotherapy with all-*trans* retinoic acid (ATRA) and a combination of anthracycline and cytarabine. After she achieved a complete remission (CR) of the APL, her bone metastases of breast cancer progressed. She received weekly paclitaxel treatments and her bone marrow function recovered. However, 9 months later, her APL relapsed; she achieved a second CR after undergoing ATRA therapy again. This patient is thought to be a rare case of secondary leukemia, since the leukemia might have been caused by hormonal therapy and regional radiation without chemotherapy.

*Key words: secondary leukemia – tamoxifen – all-*trans *retinoic acid – breast-conserving surgery – radiation*

INTRODUCTION

Chemotherapy and radiotherapy can induce secondary myelodysplastic syndrome and leukemia in patients with malignancies, and the incidences of secondary myelodysplastic syndrome and leukemia have increased (1). Systemic treatment and radiation therapy have contributed to the long-term survival of breast cancer patients, but these modalities simultaneously have the potential to cause secondary hematological malignancies. Although secondary hematological malignancies caused by chemotherapy in patients with breast cancer are quite common (2–7), the cause-relationship of hormonal agents to hematological malignancies remains controversial (8–11). We present a case of therapy-related acute

promyelocytic leukemia (tAPL) that may have been caused by regional radiation or hormonal therapy after breast-conserving surgery.

CASE REPORT

A 36-year-old female noticed a mass in her right breast and was referred to our hospital for further examination in June 2002. She was diagnosed as having stage IIA, right breast cancer and underwent a lumpectomy in August 2002. A pathological examination revealed invasive ductal carcinoma, grade 3, with no lymph node metastases. The tumor was positive for hormone-receptor and negative for HER2 over-expression. As she wished to preserve her fertility, she received neither adjuvant chemotherapy nor hormonal therapy. She received radiotherapy to her right breast (50 Gy given in 25 fractions). In January 2004, her breast cancer

For reprints and all correspondence: Chikako Shimizu, Breast and Medical Oncology Division, National Cancer Center Hospital, Tsukiji 5-1-1, Chuo-ku, Tokyo 104-0045, Japan. E-mail: cshimizu@ncc.go.jp

relapsed with multiple bone metastases and she received hormonal therapy with a gonadotropin-releasing hormone analog and tamoxifen. In April 2005, she started second-line hormonal therapy with medroxyprogesterone acetate (MPA) because of the progression of the bone metastases. In January 2006, she was emergently admitted to our hospital for fever, tender cervical lymph nodes and gingival bleeding. Her laboratory test results are shown in Table 1. A picture of a bone marrow smear is shown in Fig. 1. A cytogenetic analysis showed *t*(15;17), and both fluorescence *in situ* hybridization (FISH) and reverse transcription–polymerase chain reaction (RT–PCR) detected PML-RARα fusion DNA and its transcript, respectively. Based on these results, a diagnosis of acute promyelocytic leukemia (APL) was made. Therefore, tAPL caused by her treatment for breast cancer was suspected. She underwent induction therapy with all-*trans* retinoic acid (ATRA) for 60 days. Her clinical course is shown in Fig. 2. After the induction therapy, a bone marrow aspiration showed a hematological complete remission (CR). She then underwent consolidation therapy with mitoxantrone, cytarabine and daunorubicin. After the second course of consolidation therapy, a bone marrow aspiration revealed both cytogenetic and molecular CR. She continued receiving MPA during her treatment for APL. However, after the second cycle of consolidation therapy, bone marrow invasion developed. She was treated with weekly paclitaxel (PTX) from July 2006. Although no radiographical changes were seen on a bone scintigraphy, her complete blood count improved. Because of the peripheral edema caused by PTX,

she did not receive further therapy for breast cancer after 18 cycles of weekly PTX except for bisphosphonate.

Nine months after she finished PTX, she developed pancytopenia again in August 2007. A bone marrow aspiration revealed the relapse of APL, with positive RT-PCR findings for PML-RARα, as well as bone marrow invasion of the breast cancer cells. Re-induction therapy with ATRA for 60 days was started again because of her relatively long absence from ATRA exposure. She achieved a second hematological CR and received chemotherapy with mitoxantrone, daunorubicin and idarubicin consolidation therapy. In addition, hormonal therapy with aromatase inhibitor was given because of concerns over the progression of breast cancer. She was discharged from our hospital and remained in molecular CR.

DISCUSSION

The patient received radiation therapy to her right breast after undergoing breast-conserving surgery and tamoxifen treatment after the recurrence of her breast cancer. Generally, the risk of radiation-induced leukemia appears to be related to the volume of the bone marrow included within the radiation field, the total radiation dose and the concomitant use of chemotherapy (1,5,7). A previous study reported that the 5- and 10-year cumulative incidences for leukemia after both breast-conservative surgery and radiation for patients with stages I or II breast cancer were 0.08 and 0.8%, respectively (12), which were very low incidences and did

Table 1. Laboratory test results

Complete blood count		Biochemistry	
White blood cell count	700/μl	Albumin	4.2 g/dl
myelocyte	60/μl	Blood urea nitrogen	11 mg/dl
Stab + seg	210/μl	Creatinine	0.7 mg/dl
lymphocyte	400/μl	Sodium	144 mEq/l
promyelocyte or blast	30 μl	Potassium	3.7 mEq/l
Red blood cell count	350×10^4/μl	Chloride	105 mEq/l
Hemoglobin	11.7 g/dl	GOT	131 U/l
Hematocrit	35.0%	GPT	91 U/l
Platelet count	3.6×10^4/μl	ALP	121 U/l
		LDH	182 U/l
		C-reactive protein	2.2 mg/dl
Coagulation		Bone marrow	
PT-INR	1.77	Nucleated cell count	6.65×10^4/μl
APTT	25.5 s	Megakaryocyte count	15.3/μl
Fibrinogen	228 mg/dl	Myelocytic erythroid ratio	2.99
FDP	115.6 μg/ml	Promyelocyte + Blast	53.6%

GOT, glutamic oxaloacetic transaminase; GPT, glutamic pyruvic transaminase; ALP, alkaline phosphatase; LDH, lactate dehydrogenase, normal range: 119-229 U/l; PT-INR, prothrombin time-international normalized ratio; APTT, activated partial thromboplastin time; FDP, fibrin and fibrinogen degradation products.
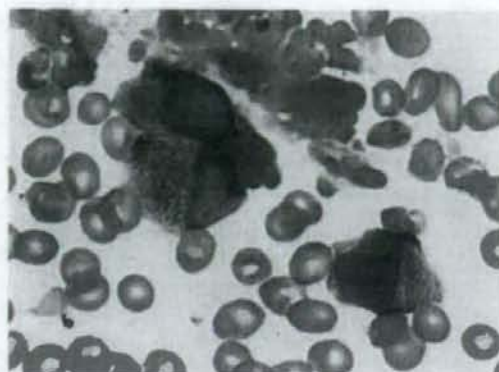
Figure 1. Bone marrow smear (May Giemsa, ×1000). Several promyelocytes with rough chromatin in their nuclei and visible Auer bodies.

not show a significant association. In the National Surgical Adjuvant Breast and Bowel Project trial, the overall risk of leukemia in patients with breast cancer who received postoperative regional radiation was 1.39% at 10 years (2). Two other large-scale, case-controlled studies demonstrated that breast cancer patients who received postoperative chest wall irradiation had an unremarkable leukemia relative risk of 0.9 [90% confidence intervals (CI), 0.4–1.8] in Germany (11) and 1.2 (90% CI, 0.6–2.1) in Connecticut (13). Although radiation therapy might have induced secondary leukemia in the present patient, this would be a rare case because the patient only received regional radiation without chemotherapy. Alkylating agents and topoisomerase II inhibitors and radiotherapy, which are useful for the treatment of breast

cancer, are known to cause secondary leukemia (2–7,14). Whether hormonal therapy is related to secondary leukemia, however, remains uncertain. Yalcin et al. reported that two breast cancer patients receiving tamoxifen developed acute leukemia (8). However, several large retrospective studies have not revealed a significant association between tamoxifen and secondary malignancies, except for endometrial cancer and colorectal cancer (9–11). In Japan, a retrospective study of secondary cancers after tamoxifen treatment in patients with breast cancer also reported that the incidence rate ratio (IRR) for secondary leukemia did not increase, but that the IRR for endometrial cancers and stomach cancers tended to increase (15).

In previous reports, the incidence of patients with tAPL ranged from 1.7 to 5.8% (16–18). One report concluded that the incidence of tAPL had increased in recent years, because 26 patients were reported between 1982 and 1991 and 80 patients were reported between 1992 and 2001 (19). Given that the overall incidence of APL has not increased, these observations suggest that either the number of patients with tAPL has increased or the disease classification of tAPL has become better recognized. Although secondary leukemia is generally considered to have aggressive characteristics and a poor prognosis because of the short duration of response, several retrospective studies have described responses to chemotherapy and the prognosis of secondary APL seem to be similar to that of *de novo* APL (19–21). Therefore, it is also important to treat patients with tAPL with the same drugs as those used for patients with *de novo* APL. Recently, ATRA and anthracycline are considered to be key drugs for *de novo* APL, while a role of cytarabine has not been confirmed (22). Because of this point of view and insufficient recovery of her bone marrow due to the bone metastases of breast cancer
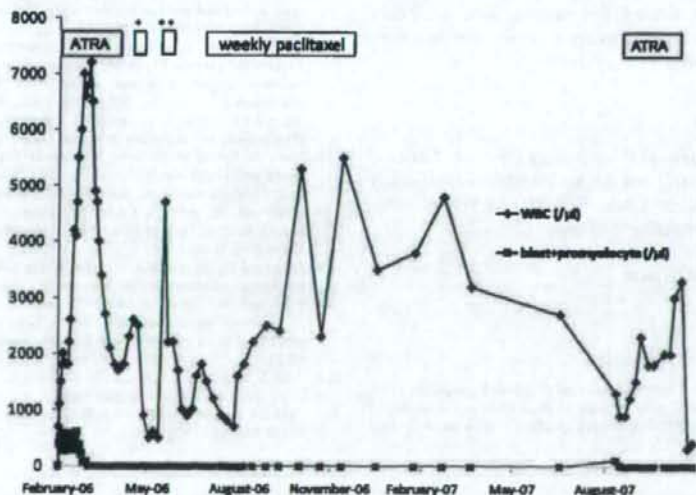

Figure 2. Clinical course. *Mitoxantrone and cytarabine, **daunorubicin; ATRA, all-*trans* retinoic acid; WBC, white blood cell.